Mineralium Deposita
https://doi.org/10.1007/s00126-024-01261-8

ARTICLE

The In-Ga-Sb association of the post-Variscan Zn-Pb-Ag vein deposit at Lautenthal, Upper Harz Mountains, Germany: sphalerite mineral chemistry

Torsten Graupner[1] · Sören Henning[1] · Simon Goldmann[1] · Sebastian Fuchs[1] · Klaus Stedingk[2] · Wilfried Liessmann[3] · Sven Birkenfeld[4]

Received: 19 December 2022 / Accepted: 10 March 2024

Abstract

The Lautenthal sphalerite-galena vein deposit is part of the world-class Upper Harz Pb-Zn-Ag district in the Harz uplift block of the Paleozoic Variscan fold belt in Germany. Its sphalerite-dominated mineral association was studied using bulk-ore chemistry, electron probe microanalysis, and laser ablation-ICP-mass spectrometry. Gallium and locally In are the main high-tech-relevant trace elements hosted by sphalerite, with up to 150 ppm Ga and up to 380 ppm In in hand-picked sphalerite samples (mean In/Zn, 0.70×10^{-3}). Ore concentrates (≤ 50 kg) contain up to 65 ppm Ga and up to 109 ppm In (mean In/Zn, 0.36×10^{-3}). Accessory Fe-Co-rich gersdorffite-1 occurs in the earlier quartz-sulfide ore stage and Sb-rich gersdorffite-2 in the later carbonate-sulfide stage. Enrichment patterns of In are either defined by overprinting textures in the Fe-richer sphalerite-1 of the earlier stage, or relate to primary growth zoning in Fe-poor sphalerite-2 of the later stage. Using the sphalerite geothermometer GGIMFis, formation temperatures (median) of sphalerite-1 were estimated at ~ 230 °C for the Lautenthal orebody and at ~ 175 °C for the Bromberg orebody, which may indicate lateral T-zonation for the earlier ore stage. Sphalerite-2 data indicate formation temperatures of ~ 185 °C (median). Copper-bearing brines of the carbonate-sulfide stage with assumed temperatures of ~ 250 °C initiated replacement of In-poor sphalerite-1 by chalcopyrite and remobilization of Zn and trace elements. Indium-rich sphalerite-2 occurs associated with calcite and fine-grained galena. A direct spatial or temporal link of ore formation to a magmatic-hydrothermal system is unlikely, which contrasts to In-rich epithermal and tin-polymetallic vein deposits worldwide.

Keywords Lautenthal · Sphalerite · Indium · Antimony · Gersdorffite · Upper Harz Mountains

Introduction

High-tech-relevant trace elements, such as indium (In) and to a lesser degree also germanium (Ge) and gallium (Ga), are commonly hosted by base metal sulfides (e.g., Ishihara et al. 2006; Sinclair et al. 2006; Cook et al. 2009, 2011; Dill et al. 2013; Murakami and Ishihara 2013; Schwarz-Schampera 2014; Jovic et al. 2015; Kumar et al. 2022, 2023) and gain rising importance in the development of innovative technologies. In the Central European Variscan fold belt in Germany, sphalerite-rich ore with significant In enrichment is so far known to occur in the shale-hosted massive sulfide deposit Rammelsberg in the Upper Harz as well as in skarn and hydrothermal vein deposits of the Erzgebirge (Schwarz-Schampera and Herzig 2002; Seifert and Sandmann 2006; Dill 2015; Bauer et al. 2019a,b; Henning et al. 2019; Korges et al. 2020).

Editorial handling: A. G. Mueller

✉ Torsten Graupner
torsten.graupner@bgr.de

[1] Federal Institute for Geosciences and Natural Resources (BGR), Stilleweg 2, 30655 Hannover, Germany

[2] Nendorfstraße 4, 38642 Goslar-Kramerswinkel, Germany

[3] Institute of Disposal Research, Clausthal University of Technology, Adolph-Roemer-Straße 2A, 38678 Clausthal-Zellerfeld, Germany

[4] Clausthal University of Technology, CUTEC Institute, Leibnizstraße 23, 38678 Clausthal-Zellerfeld, Germany

Published online: 13 April 2024

Numerous Pb-Zn-Ag deposits have been mined in the Upper Harz Mountains for more than 1000 years; the total production of the Rammelsberg deposit was estimated at 2.2 Mt Pb, 4.6 Mt Zn, 0.5 Mt Cu, and > 4 kt Ag, whereas that of the vein-type deposits was 1.9 Mt Pb, 1.5 Mt Zn, and > 5 kt Ag (e.g., Klockmann 1893; Kraume 1955, 1958; Buschendorf et al. 1971; Sperling and Stoppel 1979; Stoppel et al. 1983; Brinckmann et al. 1986; Stedingk 1986, 2012, 2021; Möller and Lüders 1993; Müller 2022). However, there are few studies on ore genesis and exploration potential using modern analytical approaches. In particular, in situ trace element analysis of ore minerals (e.g., laser ablation-ICP-mass spectrometry) and investigation of accessory minerals in host rocks and veins using (field emission) scanning electron microscopy are lacking. Recent overview studies, almost exclusively on historical collection specimens (e.g., Graupner et al. 2019; Henning et al. 2019; Schirmer et al. 2020), revealed that vein-type base metal deposits in the Upper Harz Mountains locally host sphalerite with significant concentrations of In. A first evaluation of the data has shown that such In-bearing veins share characteristics with their well-known equivalents in the Erzgebirge and in the mostly sub-volcanic rocks in Bolivia (e.g., Seifert and Sandmann 2006; Murakami and Ishihara 2013).

The sphalerite-dominated Lautenthal deposit (Zn/Pb ratio of produced metal: 2.9; Stedingk 2012) in the northwestern Upper Harz mining district, located ~ 10 km SW of the Rammelsberg deposit, was among the recently identified In-bearing vein systems. Newly compiled geologic field observations as well as mineralogical and trace element geochemical data for this deposit are presented here. Trace element (e.g., In, Ga, Ge, Sb, Cu, Sn) characteristics of sphalerite are used to put constraints on ore formation. Special focus is on the accessory ore minerals and their potential for an improved classification of the polycyclic mineralization. Finally, the sphalerite data are comparatively discussed with worldwide equivalents.

Regional geology

The Harz Mountains in central Germany are part of the Rhenohercynian zone of the Variscan orogenic belt and are for the most part composed of siliciclastic Paleozoic strata intruded by granites and minor gabbro (Fig. 1). The Early Paleozoic to Lower Carboniferous package strongly varies in thickness from about 2 km in the south-eastern Harz Mountains up to about 6 km in the north-western part (Upper Harz Mountains), and largely consists of flysch-like sediments (greywacke), shale, conglomerates, limestone reefs, and locally metabasalt (Franke and Oncken 1995; Franke 2000; Huckriede et al. 2004). During the Variscan Orogeny, the sediment-filled troughs were deformed into a fold and thrust belt. Intrusion of the post-orogenic Brocken, Oker, and Ramberg granites and

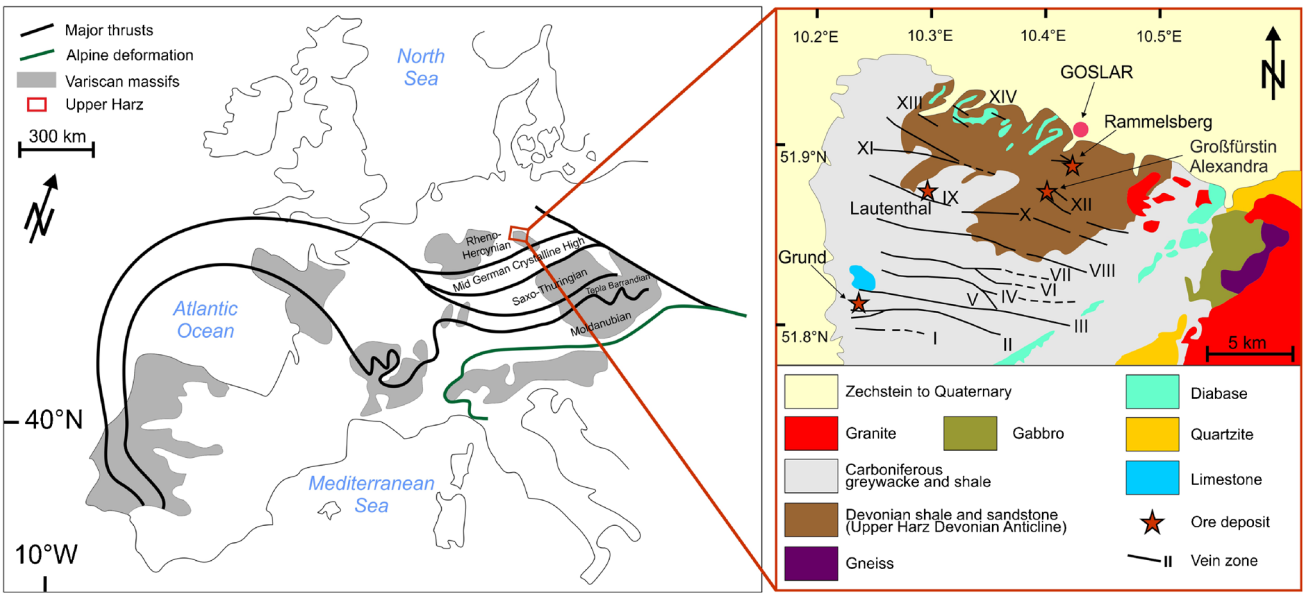

Fig. 1 Position of the Harz Mountains in the European Variscides (modified from McKerrow et al. 2000) and schematic geological map of their western parts (Upper Harz and western parts of the Middle Harz) showing the position of relevant base metal deposits. Important fault systems of the Upper Harz district (after Jacobsen and Schneider (1951) and Jacobsen et al. (1971)): I—Laubhütte fault system; II—Silbernaal fault system; III—Rosenhof fault system; IV—Zellerfeld fault system; V—Burgstätte fault system; VI—Haus Herzberg fault system; VII—Spiegeltal fault system; VIII—Bockswiese fault system; IX—Lautenthal fault system; X—Hahnenklee fault system; XI—Gegental fault system; XII—Schleifsteintal fault system; XIII—Burghagen fault system; XIV—Heimberg-Dröhneberg, Beste Hoffnung and Todberg fault systems

the Harzburger gabbro is dated to Early Permian (e.g., 297 to 283 Ma U–Pb zircon, Rb–Sr and K–Ar mineral ages; Baumann et al. 1991; Zech et al. 2010).

The multiple interconnecting fault systems in the Upper Harz Mountains (Figs. 1 and 2) consist of steeply SSW-dipping fracture zones with Hercynian strike (WNW-ESE direction) that formed as a combination of Late Variscan tectonics and Mesozoic wrench-faulting (Behr et al. 1987). A curved fault pattern including merging and branching lodes is visible for the Upper Harz mining district (Fig. 2). Along the boundary of the Harz, the folded Paleozoic strata are discordantly overlain by Lower Permian rocks (Upper Rotliegend) and the evaporite sequence of the Zechstein, with Zechstein transgression conglomerate and the Copper Shale ("Kupferschiefer") at its base (Upper Permian). Late Cretaceous intraplate shortening in Central Europe produced uplift of the Harz Mountains with a final vertical displacement of 5 to 7 km and erosion of Permian and Mesozoic rocks (e.g., von Eynatten et al. 2008).

Geology of the Upper Harz block

The major structural units in the study area are the Upper Harz Devonian Anticline (UHDA) and the Carboniferous Clausthal Culm Fold Zone (CCFZ), which are bordered to the SE by the Devonian Upper Harz Diabase Range (Fig. 1). The oldest stage of the stratigraphic succession is represented by the Lower Devonian (Upper Emsian stage) Kahleberg Sandstone, which is composed of 1000 m of sandstone, quartzite, and shale and forms the core of the UHDA (Fig. 2). The overlying Middle to Upper Devonian pelitic and partly carbonate-bearing sedimentary rocks (e.g., Wissenbach Shale; Figs. 2 and 3) locally strongly vary in thickness reaching up to 1000 m, with intercalated layers of tuff. The stratiform Pb-Zn-Cu-barite orebodies of the Rammelsberg massive sulfide deposit are emplaced within this succession (Eifelian stage of the Middle Devonian; ca. 390 Ma; Fig. 2). Following the generally pelitic

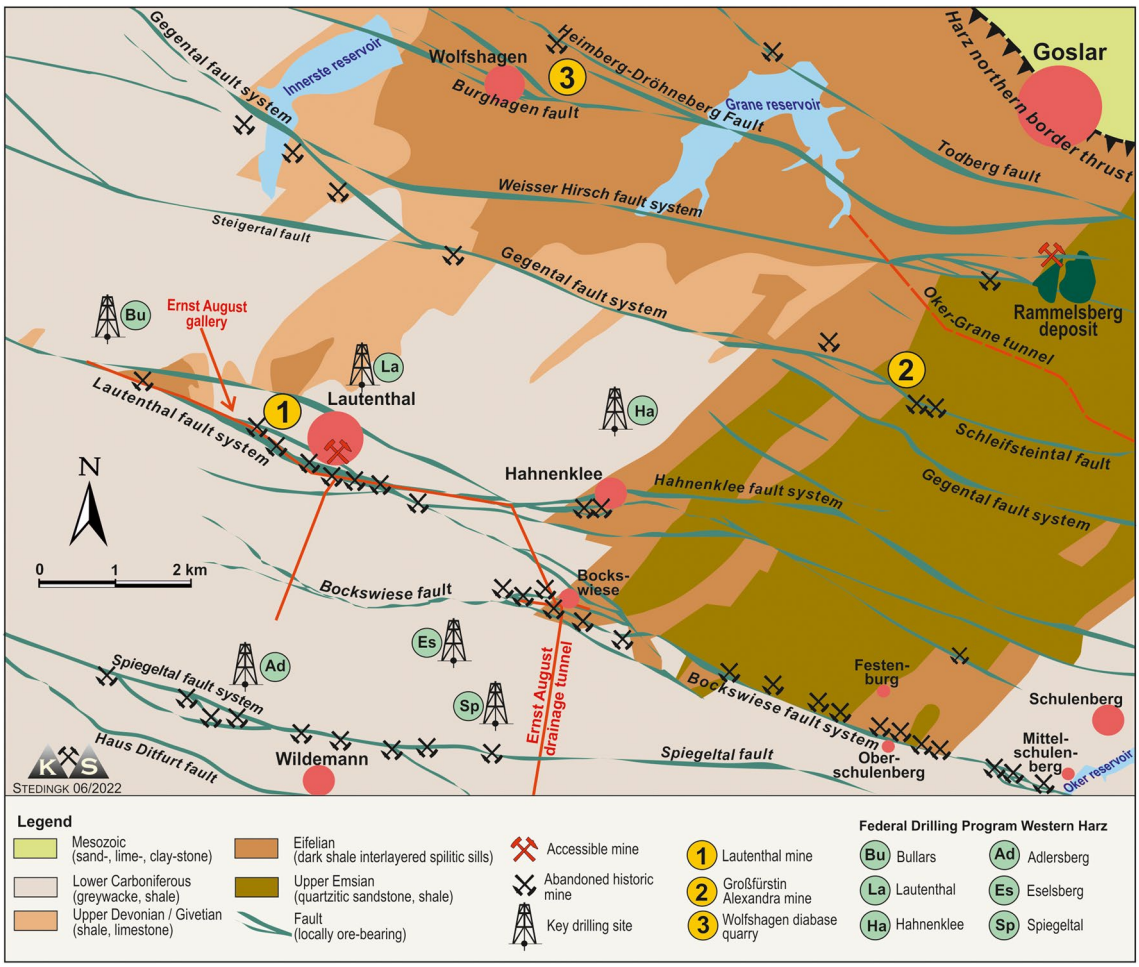

Fig. 2 Schematic geological map of the northern section of the Upper Harz Mountains showing the position of the studied mines. The drilling locations Bullars, Lautenthal, and Hahnenklee just N of Lautenthal enable access to cores containing sequences of Devonian up to Lower Carboniferous rocks (Brinckmann et al. 1986)

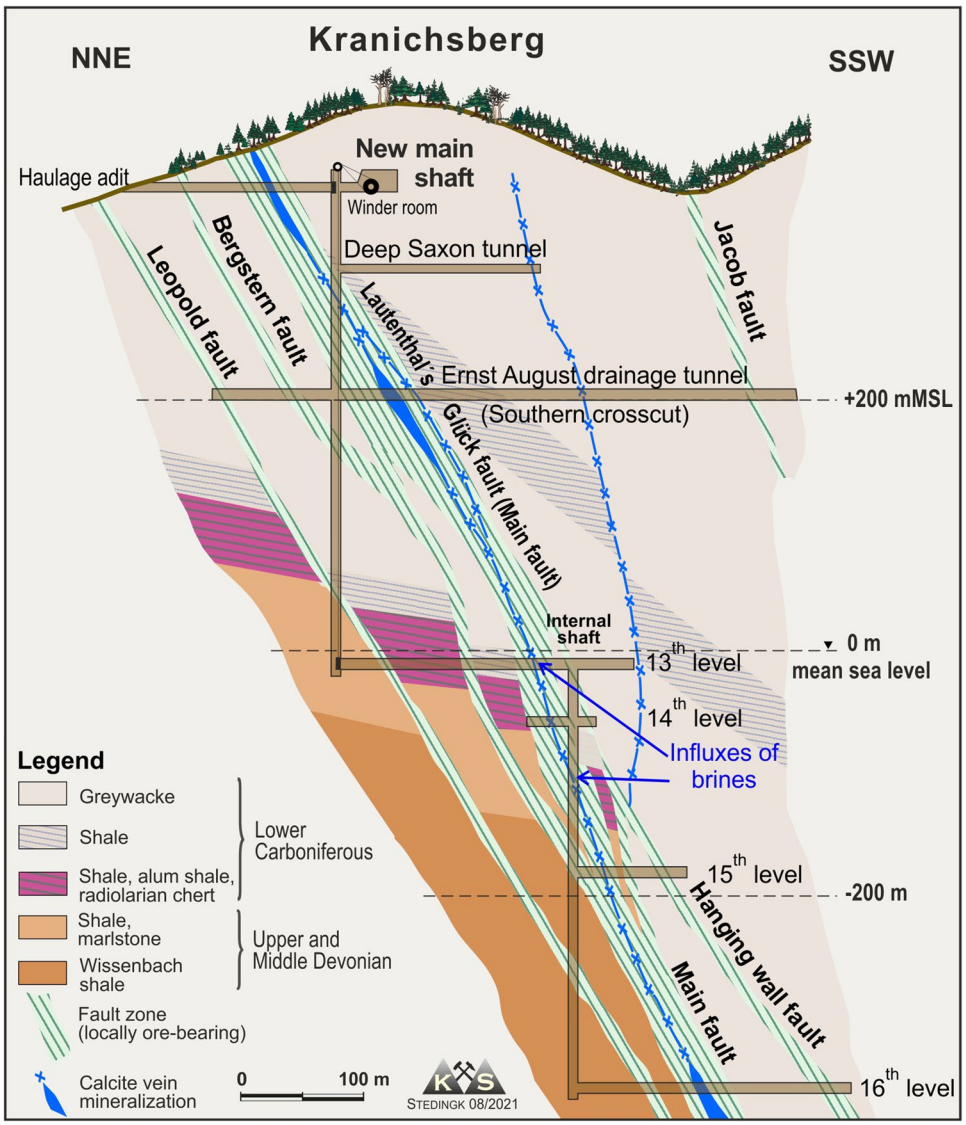

Fig. 3 Vertical NNE-SSW cross-section through the Lautenthal fault system close to the location of the New main shaft of the Lautenthal's Glück mine (for position of the shaft see Fig. 4a). Data sources: Kraume (1958), Stedingk (2012)

shales, the prevailing sediments from the Upper Devonian up to the Lower Carboniferous are clastic flysch sediments of the CCFZ composed of greywacke, shale, and radiolarian chert (lydite; Figs. 1, 2, and 3).

The Lautenthal fault system is the northernmost fault system of economic importance in the Upper Harz (IX in Fig. 1), followed S by the similar Silbernaal (Grund) and Burgstätte (Clausthal) fault systems (II-V in Fig. 1). It initiates NE of Seesen and crosscuts in eastern direction shales and greywacke of Lower Carboniferous age and Middle to Upper Devonian shales (Fig. 3). Lateral movement of the southern hanging wall occurred into south-eastern direction along the faults. The system cuts and displaces a N-S striking kersantite (lamprophyre) dyke, which is discussed to be Upper Carboniferous to Lower Permian (Rotliegend) in age (Schriel 1954; Gabert 1958). However, the dyke has not been dated by radiometric methods. The stepwise downward displacement of the Lower Carboniferous strata starting from the footwall (NNE) towards the hanging wall (SSW) of the Lautenthal fault system (by ~ 500 m in total) is illustrated by a vertical NNE-SSW cross-section through the fault system (Fig. 3).

For the Grund vein deposit (Fig. 1), which is structurally and paragenetically similar to the Lautenthal deposit, Rb–Sr ages on illite provide the only age dates available for the Upper Harz Zn-Pb-Ag veins. Using these age data, the formation of the vein-type ores was attributed to two events in the Triassic (238 ± 20 Ma) and Lower Jurassic (178 ± 9 Ma; Boness et al 1990); however, the data were later re-interpreted using a mixing model resulting in one Lower Jurassic age (183 Ma; Lüders and Möller 1992; Haack and Lauterjung 1993). In the Grund mine, ~ 19.1 Mt ore containing 740 kt Zn and 1.1 Mt Pb (Zn/Pb, 0.7) was produced until 1992 and remaining resources are ~ 5 Mt ore containing ~ 220 kt Zn, ~ 200 kt Pb, and ~ 180 t Ag (Stedingk 2021).

The Lautenthal base metal vein deposit

The estimated total production of the Lautenthal mines from 1620 to 1946 was 4.2 Mt ore at a grade of 6.7% Zn and 2.3% Pb containing 280 kt Zn and 97 kt Pb (Stedingk 2012). The economically most important vein of the deposit is the Lautenthal vein (Main fault; Figs. 3 and 4a, b). The Leopold and Bergstern faults, occurring close to its footwall contact, as well as the Jacob fault to the S of the Main fault (Fig. 3), are occasionally mineralized with Zn-Pb ore. A more intense development of the base metal sulfide ores, also extending to greater depth, seems to characterize the Lautenthal orebody, when compared to the Bromberg one (Fig. 4b). In the Lautenthal orebody, the Lautenthal vein splays up into three branch veins ("Trümer") for ~ 2 km with massive ore (Fig. 4a). The Lautenthal's Glück branch vein was the main target of mining here. Zoning with depth was not observed in the latter orebody; neither a galena-siderite-barite zone exists on top of the sphalerite-dominated ore, nor indications for a chalcopyrite-richer zone at greater depth were found (Sperling and Stoppel 1979). Following eastwards, the branch veins re-unite into a barren fault zone, which extends

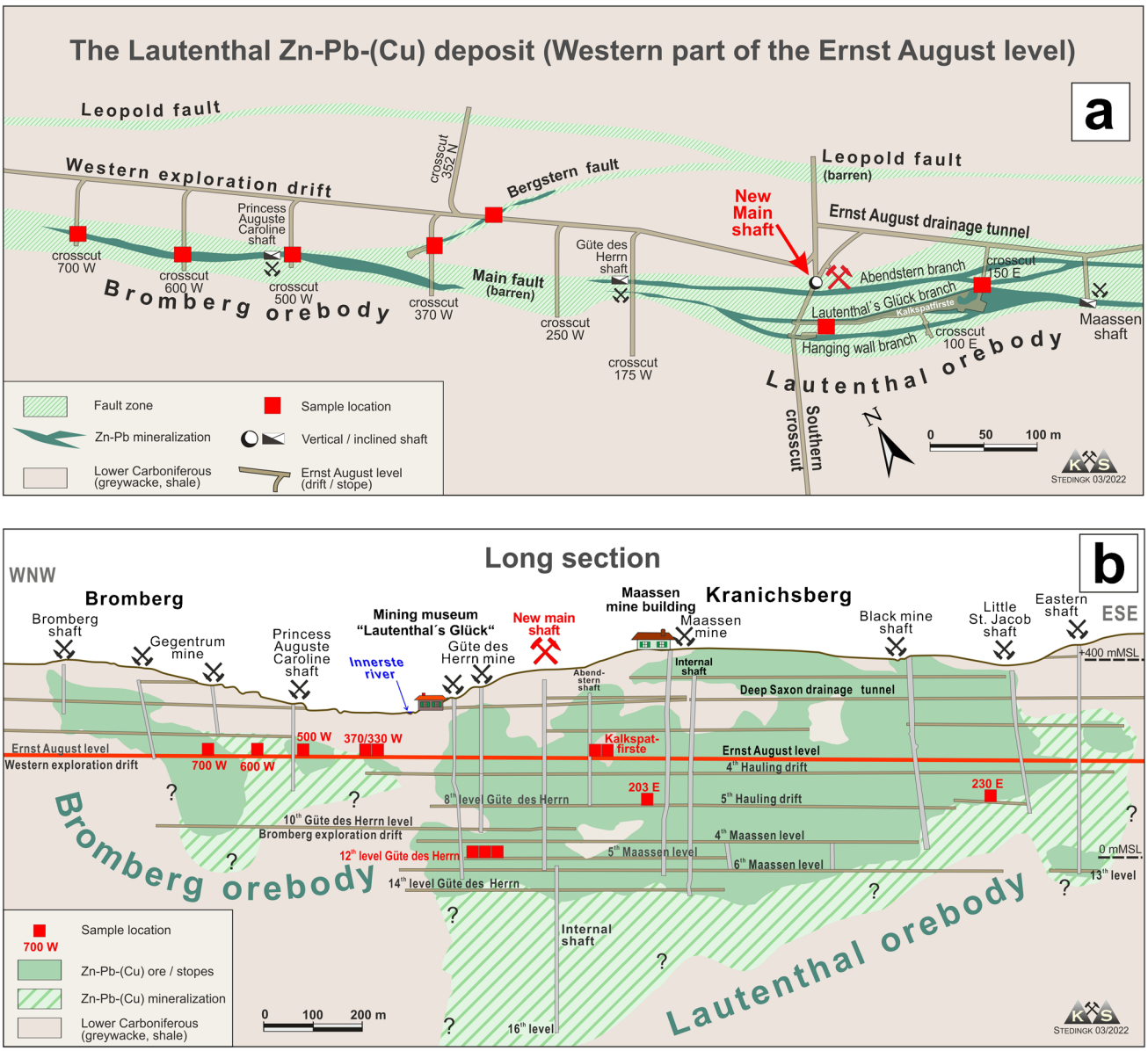

Fig. 4 **a**, **b** Schematic overview maps for the Lautenthal vein deposits. **a** Mine plan of the western and central part of the Lautenthal's Glück mine at the Ernst August gallery level (+200 mMSL). **b** Vertical WNW-ESE cross-section along the Lautenthal fault system (long section of the orebodies projected onto a vertical plane). MSL, mean sea level

towards the village of Hahnenklee where it crosscuts the Kahleberg sandstone (Fig. 2).

Four hydrothermal pulses (stages) are commonly distinguished for the post-Variscan base metal vein deposits of the Upper Harz Mountains (Sperling 1973; Lüders et al. 1993b). A pre-ore stage followed by two main ore stages with massive precipitation of base metal-silver ores are described for the Lautenthal deposit (e.g., Sperling and Stoppel 1979). The latter stages resulted from repeated opening of the vein fractures by movement along listric faults. The quartz-sulfide stage (main ore stage I; Table 1), with common occurrence of massive, banded, and breccia ore types in up to several-meters-wide ore veins, and the subsequent carbonate-sulfide stage (main ore stage II) with a predominance of breccia ore. By volume and economic importance, base metal ore of the quartz-sulfide stage clearly dominates over the later stage ore (Sperling and Stoppel 1979). Ore veins of the carbonate-sulfide stage frequently show a complex internal structure and calcite can reach up to 12 m thickness in the so-called Kalkspatfirste (Lautenthal orebody; e.g., Stedingk 2012). A later siderite-dominant sub-stage of this ore stage is developed in other Upper Harz Mountains vein deposits, but not present in the orebodies at Lautenthal. However, Sperling and Stoppel (1979) found siderite veinlets outside of the orebodies (Table 1). The post-ore stage has no economic significance in the deposit.

The economically most important ore minerals of the Lautenthal deposit were sphalerite with mostly moderate to low Fe contents, Ag-bearing galena, and minor chalcopyrite, similar to most Pb-Zn-Ag vein deposits in the Upper Harz. The Lautenthal and Bergstern veins show mostly a predominance of sphalerite over galena. Light brownish to brown sphalerite was found to be essentially free of fine-grained mineral inclusions (e.g., no "chalcopyrite disease"; cf. Barton and Bethke 1987). However, one deep to black brown sphalerite sample of unknown origin (probably from a deep mining level of the Lautenthal orebody) was previously described to contain numerous dust-like chalcopyrite inclusions that outline crystallographic patterns of the mineral (Buschendorf and Hüttenhain 1971). The ore grade at Lautenthal is highly variable along strike and depth of individual veins.

Samples and analytical methods

Seven underground vein outcrops located at the level of the Ernst August gallery were investigated in the Lautenthal deposit (Table ESM 1; Figs. 4a, b). The Lautenthal vein (Main fault) was studied at the crosscuts 500 m West, 600 m West, and 700 m West (Bromberg orebody; Fig. 4a, b). The Bergstern vein was accessible at 330 m West and 370 m West of the same orebody. Within the Lautenthal orebody, the Lautenthal's Glück branch vein was studied using outcrops in the Kalkspatfirste at ~ 100 m East (Fig. 4a, b). Collection specimens used from the Lautenthal and the Jacob

Table 1 Summary of the observed ore, gangue, and accessory minerals in the studied vein outcrops of the Lautenthal deposit with addition of data from Sperling and Stoppel (1979) for inaccessible parts of the mine workings

Mineral	Quartz-sulfide stage (main ore stage I)	Carbonate-sulfide stage (main ore stage II)		
		Quartz-dominated sub-stage	**Calcite-dominated sub-stage**	**Siderite-bearing assemblage (occurrence west of the Bromberg orebody*)**
Galena	**Galena-1**	Galena-2a	Galena-2b	*Galena*
Sphalerite	**Sphalerite-1**	Sphalerite-2a	Sphalerite-2b	*Sphalerite*
Chalcopyrite	Chalcopyrite*	Chalcopyrite		*Chalcopyrite*
Pyrite	Pyrite	Pyrite		
Marcasite				*Marcasite(?)*
Tetrahedrite		*Tetrahedrite-(Zn)*		
Freibergite			*Freibergite-(Zn)*	
Bournonite			*Bournonite*	
Gersdorffite	*Gersdorffite-1*	*Gersdorffite-2*		
Arsenopyrite	*Arsenopyrite-1*	*Arsenopyrite-2*		
Quartz	**Quartz**	**Quartz**	Quartz	Quartz
Calcite	Calcite	Calcite	**Calcite**	Calcite
Siderite			*Siderite*	**Siderite**
Synchysite-(Ce,Nd)			*Synchysite-(Ce,Nd)*	

*Data are from Sperling and Stoppel (1979); bold—major minerals; normal—minor minerals; italic—accessory minerals

veins are listed in Table ESM 1. Altogether, 35 hand specimens were studied from Lautenthal using ~ 40 polished centimeter-sized slabs. Furthermore, millimeter-sized sphalerite grains of eight samples were hand-picked under a binocular microscope. The separated fractions have sulfide contents between 75 and 99 wt%. Their bulk chemistries are determined to check the relevance of the micro-analytical spot measurements with regard to the trace element composition of the mineral. Additionally, seven moderate volume sphalerite-enriched ore concentrates (~ 0.5 to > 50 kg each) were prepared by hand cobbing ore piles with up to decimeter-sized material (A. Haas, pers. comm.; Graupner et al. 2019). The material derives from three large volume samples (> 200 kg each) from the Lautenthal vein at 500 m West and the footwall and central branches of the same vein at 700 m West (Table ESM 1). The first two outcrops are attributed to the quartz-sulfide stage, whereas the central branch at 700 m West contains substantial amounts of carbonate-sulfide stage ore.

Energy-dispersive X-ray fluorescence spectrometry major and minor element mapping (µ-EDXRF) was carried out using the M4 Tornado by Bruker at BGR to obtain an overview on the textural characteristics and the mineral proportions of larger rock slices (maximum size, 16 × 20 cm). Mineral distribution maps were obtained by supervised classification using the "Spectral Angle Mapper" algorithm (Nikonow and Rammlmair 2017).

Scanning electron microscope (SEM) investigations of carbon-coated polished sections were carried out at BGR using a MLA650F (Quanta 650 FEG system; FEI Company). The system was equipped with two energy-dispersive X-ray detectors (XFlash Detector 5030, Silicon Drift Detector; Bruker Nano) for semi-quantitative element analysis.

In situ laser ablation-inductively coupled plasma-mass spectrometry (LA-ICP-MS) was used applying a Plasma-Quant Elite quadrupole ICP-MS by Analytik Jena coupled to a 213-nm laser ablation system (LSX-213 G2 + by CETAC Technologies). The laser system was adjusted to ablate round 40 µm spots using a fluence of 8 J/cm^2 at 20 Hz for 15 s. Prior to each ablated spot, a gas blank was monitored for 15 s. On each polished sample 30 to 50 spots on sphalerite were analyzed. Helium was used as the carrier gas (0.4 l/min). Argon was used as cool, auxiliary, and sample gas of the ICP-MS and the gas flow rates were adjusted to 9.0, 1.35, and 1.04 l Ar/min, respectively. The isotopes ^{34}S, ^{44}Ca, ^{51}V, ^{52}Cr, ^{55}Mn, ^{56,57}Fe, ^{59}Co, ^{60}Ni, ^{63,65}Cu, ^{66}Zn, ^{71}Ga, ^{74}Ge, ^{75}As, ^{77,78,82}Se, ^{83}Kr, ^{95}Mo, ^{107}Ag, ^{111}Cd, ^{115}In, ^{117,118}Sn, ^{121}Sb, ^{126}Te, ^{137}Ba, ^{205}Tl, and ^{208}Pb were monitored by the ICP-MS using a dwell time of 10 ms for each isotope. The average limits of detection of the method (LODs) for selected elements are listed in Table ESM 2. The mineral chemistry of sphalerite was determined for ~ 35 samples with > 1000 LA-ICP-MS measurement spots (Table ESM 2).

Electron probe microanalysis (EPMA) was performed on carbon-coated sections using a JEOL JXA-8530F Hyperprobe at BGR. The quantitative analysis of the major, minor, and trace element compositions of sphalerite, galena, chalcopyrite, marcasite, gersdorffite, arsenopyrite, calcite, tetrahedrite, and bournonite were conducted by single spot analyses using wavelength-dispersive X-ray spectrometry (WDS) with acceleration voltages ranging from 12 kV (carbonate) to 25 kV (sulfides) and beam currents ranging from 20 nA (carbonate) to 80 nA at spot sizes of about 1–2 µm (sulfides). The LOD for Ge (30 ppm), Ga (23 ppm), and In (24 ppm) are higher compared to those of the LA-ICP-MS. Semi-quantitative mapping of major and trace element concentrations in rectangular segments (up to 4 × 4 mm in size) of sphalerite grains was carried out using the energy-dispersive X-ray spectrometry (EDS; Zn Kα, S Kα, Fe Kα) and WDS methods (Cd Lα, Cu Kα, In Lα, Ga Kα, Sb Lα) with variable spot sizes ranging from 0.4 to 6.2 µm depending on the step size for the respective mapping area.

Sodium peroxide fusion was used to prepare the hand-picked sphalerite samples for analysis (Actlabs-Activation Laboratories Ltd., Canada). Major elements (Cu, Fe, Zn, Pb, S) were analyzed by inductively coupled plasma-optical emission spectrometry (ICP-OES, assays) and trace elements (Ga, Ge, In, Sn, Cd) by ICP-MS. The limits of detection for the trace elements are between 0.2 and 2.0 ppm. Moderate volume ore concentrates were crushed and subsequently milled. The major and trace elements were either analyzed by ICP-OES or by a combination of ICP-OES and ICP-MS (In).

Results

Ore mineralogy of hydrothermal stages at Lautenthal

Pre-ore stage Intense fluid-rock interaction during this stage is reflected by local silicification of wall rocks and formation of commonly zoned dolomite-ankerite (lenses and veinlets). Euhedral pyrite overgrowing earlier framboidal aggregates in the altered rocks close to veins and in the vein selvages is accompanied by quartz, calcite, rutile, and less commonly apatite. These features of early hydrothermal fluid overprint are common in the studied outcrops of the deposit, and often outline vein margins.

Quartz-sulfide stage (main ore stage I) Major base metal ore minerals in the massive, banded, and breccia ore types are moderately Fe-bearing sphalerite-1 and coarse-grained galena-1 with minor pyrite and chalcopyrite (Table 1 and 2); quartz is the dominant gangue mineral. Light brownish

Table 2 Summary of EPMA results of selected base-metal sulfide, Fe-Co–Ni sulfarsenide, and sulfosalt analyses for samples from different ore stages of the Lautenthal deposit

Ore stage/mineral	Sample	S (wt%)	Fe (wt%)	Co (wt%)	Ni (wt%)	Cu (wt%)	Zn (wt%)	As (wt%)	Ag (wt%)	Cd (wt%)	Sb (wt%)	Pb (wt%)	Ge (ppm)	Ga (ppm)	In (ppm)	Total (wt%)
Quarz-sulfide stage																
Sphalerite-1	15-LTG-5–3	34.52	3.32	< 0.004	n.a	0.02	63.33	< 0.03	< 0.04	0.09	< 0.03	n.a	< 88	< 65	< 61	101.29
Galena-1	17-LTG-7	13.64	< 0.02	< 0.006	< 0.009	< 0.03	< 0.03	< 0.07	< 0.03	< 0.04	< 0.02	86.92	< 224	< 110	< 74	100.56
Gersdorffite-1	17-LTG-12	18.74	5.22	1.39	27.03	< 0.05	< 0.04	46.01	< 0.05	n.a	0.12	< 0.07	n.a	n.a	n.a	98.50
Arsenopyrite-1	17-LTG-3	21.90	21.33	7.59	4.86	< 0.05	< 0.03	43.59	< 0.05	n.a	< 0.04	< 0.07	n.a	n.a	n.a	99.27
Carbonate-sulfide stage																
Sphalerite-2a	17-LTG-20	33.70	1.52	< 0.004	n.a	0.05	65.48	< 0.03	< 0.02	0.33	< 0.02	n.a	< 102	< 67	625	101.15
Sphalerite-2b	18-LTG-1d	33.11	0.65	< 0.004	n.a	0.39	65.22	< 0.03	< 0.04	< 0.08	< 0.03	n.a	< 88	103	4,360	99.85
Galena-2b	18-LTG-1e	13.82	< 0.02	< 0.006	< 0.009	< 0.03	< 0.03	< 0.07	0.06	0.04	0.54	84.72	< 224	< 130	< 73	99.18
Chalcopyrite	17-LTG-16	35.15	30.10	< 0.02	< 0.02	34.48	< 0.03	< 0.04	< 0.04	n.a	< 0.04	< 0.08	n.a	n.a	n.a	99.73
Tetrahedrite-(Zn)	17-LTG-18	23.86	2.11	< 0.005	< 0.007	34.90	5.89	< 0.05	3.76	< 0.04	29.17	< 0.03	< 157	< 77	< 86	99.69
Freibergite-(Zn)	14-LTG-2-1a	23.49	2.01	< 0.005	< 0.007	23.99	4.79	< 0.05	17.93	< 0.07	27.53	0.06	< 162	< 81	< 135	99.79
Bournonite	14-LTG-2–2	19.28	< 0.05	< 0.02	< 0.03	12.84	< 0.05	< 0.05	< 0.06	n.a	24.94	41.97	n.a	n.a	n.a	99.03
Gersdorffite-2	17-LTG-16	19.32	0.17	0.90	34.04	< 0.05	0.18	38.61	< 0.05	n.a	6.19	< 0.06	n.a	n.a	n.a	99.48
Arsenopyrite-2	17-LTG-3	21.53	33.59	0.13	0.03	< 0.03	0.11	42.64	< 0.02	n.a	0.94	< 0.02	n.a	n.a	n.a	98.97
Post-ore stage																
Sphalerite-3	17-LTG-14	32.59	0.21	< 0.004	< 0.006	< 0.02	66.73	< 0.04	< 0.02	0.68	< 0.02	< 0.03	< 140	< 76	< 61	100.25
Marcasite-3	17-LTG-14	52.26	44.76	< 0.005	< 0.005	0.06	< 0.02	0.10	1.12	< 0.03	1.24	0.93	< 130	< 65	< 65	100.47

n.a. not analyzed

to brown sphalerite-1 commonly occurs as coarser-grained massive aggregates, in banded textures, or as fragmented grain aggregates in brecciated vein segments (Fig. 5a). It is more frequent in the Lautenthal veins than later sphalerite generations. Sphalerite-1 shows primary oscillatory growth zoning and/or sector zoning and grains from the studied mining levels (Fig. 4b) were essentially free of fine-grained oriented mineral inclusions. Most samples from the Lautenthal orebody contain sphalerite-1 with higher Fe contents (Table ESM 2), when compared to material from the Bromberg orebody. Along vein selvages and inside of or adjacent to wall rock fragments in brecciated ore, minor to moderately As-, Ni-, and Co-bearing early pyrite commonly acted as nucleus for the crystallization of gersdorffite-1 overgrowths (Fig. 5c; arsenopyrite-1 overgrowth is scarce) or was occasionally replaced by gersdorffite-1 to variable degrees (cf. Figure 5d, e). Sphalerite-1 and galena-1 occur in close spatial association with zoned quartz that hosts gersdorffite-1. However, the base metal sulfides are often devoid of gersdorffite-1 inclusions. The most important minor elements in gersdorffite-1 are Fe and Co (Table 2), with the first one showing the strongest variability in zoned crystals (Fig. 5f). Mineral associations, characterized by significant replacement of moderately Fe-bearing sphalerite-1 by later chalcopyrite (Fig. 5b), are well documented especially for breccia ore from the Lautenthal orebody. Occasionally, small remnants of replaced sphalerite are left behind within lenticular or irregularly formed chalcopyrite aggregates. Massive vein calcite, which is often embedding such sphalerite-1-chalcopyrite mineral associations, is attributed to the subsequent carbonate-sulfide stage.

Carbonate-sulfide stage (main ore stage II) Ore formation within this stage is commonly initiated by reactivation of fault structures hosting older stage ore and is characterized by multiple stages of deformation and mineral precipitation (e.g., cockade breccia textures). This frequently resulted in formation of complex vein outcrops (e.g., Fig. 6(a)) accessible along the Lautenthal and Bergstern veins at the Ernst August gallery level. The ore stage is sub-divided into a quartz-dominated and a calcite-dominated sub-stage (Table 1). Elevated galena-2 contents in the sphalerite-2-galena-2 ore occur spatially confined to the westernmost vein outcrops of the deposit. Minor to locally moderate quantities of chalcopyrite, as well as minor to accessory amounts of the Cu-Sb-Ag sulfosalts tetrahedrite-(Zn) and freibergite-(Zn) (Fig. 5i, l), bournonite (Fig. 5l) and the Fe-Co-Ni sulfarsenides gersdorffite-2 and arsenopyrite-2 (Fig. 5i–k, m–o) are also present (Table 1 and 2). The minor element composition of the gersdorffite-2 grains is significantly different to the type 1 grains. Whereas Fe and Co are rather low in gersdorffite-2, it commonly contains significant Sb concentrations (maximum value ~ 10 wt% Sb; Table 2). Sphalerite-2a typically appears in almost mono-mineralic ribbon-like textures in zoned quartz stringers, whereas sphalerite-2b occurs as fine-grained intergrowth with chalcopyrite ± fahlore and late galena-2b or as coarser-grained anhedral aggregates (Fig. 5h). Both sphalerite generations (sphalerite-2a and sphalerite-2b) commonly have rather low Fe contents (Table 2), show light to middle brown colors, display intense primary oscillatory growth zoning and sector zoning, and are devoid of fine-grained oriented mineral inclusions. Fine-grained galena-2a typically forms net-like textures in multiple layers of zoned quartz by the arrangement of its fine grains (Fig. 6(b, c)). Galena-2b is present as late anhedral grains and aggregates in cavities between calcite and sphalerite-2b (Fig. 5h) or forms replacement textures enclosing fragments of partly replaced sulfides (Fig. 5l). In calcite-rich vein segments, fine veinlets and nests of galena-2 and tetrahedrite occur in chalcopyrite; both minerals replace chalcopyrite (Fig. 5i).

Post-ore stage This stage is characterized by local redistribution and recrystallization of vein minerals. Minor amounts of sphalerite-3, galena-3, and marcasite-3 occur on veinlets.

Relationship between main ore stages I and II The relationship between these ore stages is illustrated in the complex vein outcrop from the central branch of the Lautenthal vein in the Bromberg orebody described in the following section (Fig. 6(a)). The exposed wall rocks are composed of folded and deformed massive greywacke and shale (Lower Carboniferous IIIβ; Sperling and Stoppel 1979). Close to the NNE vein margin, several quartz-galena-2a-sphalerite-2a stringers of the quartz-dominated sub-stage of the carbonate-sulfide stage cut moderately Fe-bearing banded sphalerite-1 of the quartz-sulfide stage (Fig. 6(b)). Ribbon-like sphalerite-2a in the center of cutting stringers is rimmed by gersdorffite-2 bearing quartz (not shown). The southern segment of the vein outcrop (Fig. 6(a)) is dominated by calcite-sphalerite-2b(-quartz) ore attributed to the calcite-dominated sub-stage of the carbonate-sulfide stage. The age relationship between the quartz-galena-2a-sphalerite-2a stringers and the calcite-dominated sub-ore stage is clarified by the presence of stringer fragments, which are tectonically rotated and embedded in massive calcite of the younger sub-stage (Fig. 6(c)). A profile covering half of the vein (Fig. 6(d)) provides a brief overview on the ore textures of the calcite-dominated sub-ore stage. It derives from the continuation of the vein shown in Fig. 6(a) on the roof of the crosscut; quartz-sulfide stage sphalerite-1 is lacking here. A marginal brecciated zone (a in Fig. 6(d)) is followed by massive calcite of the carbonate-sulfide stage, making up most of the precipitates towards the vein center (b to d in Fig. 6(d)). Cavities remaining in the center after calcite precipitation are filled mainly by anhedral sphalerite-2b (Figs. 5h, 6(a); e

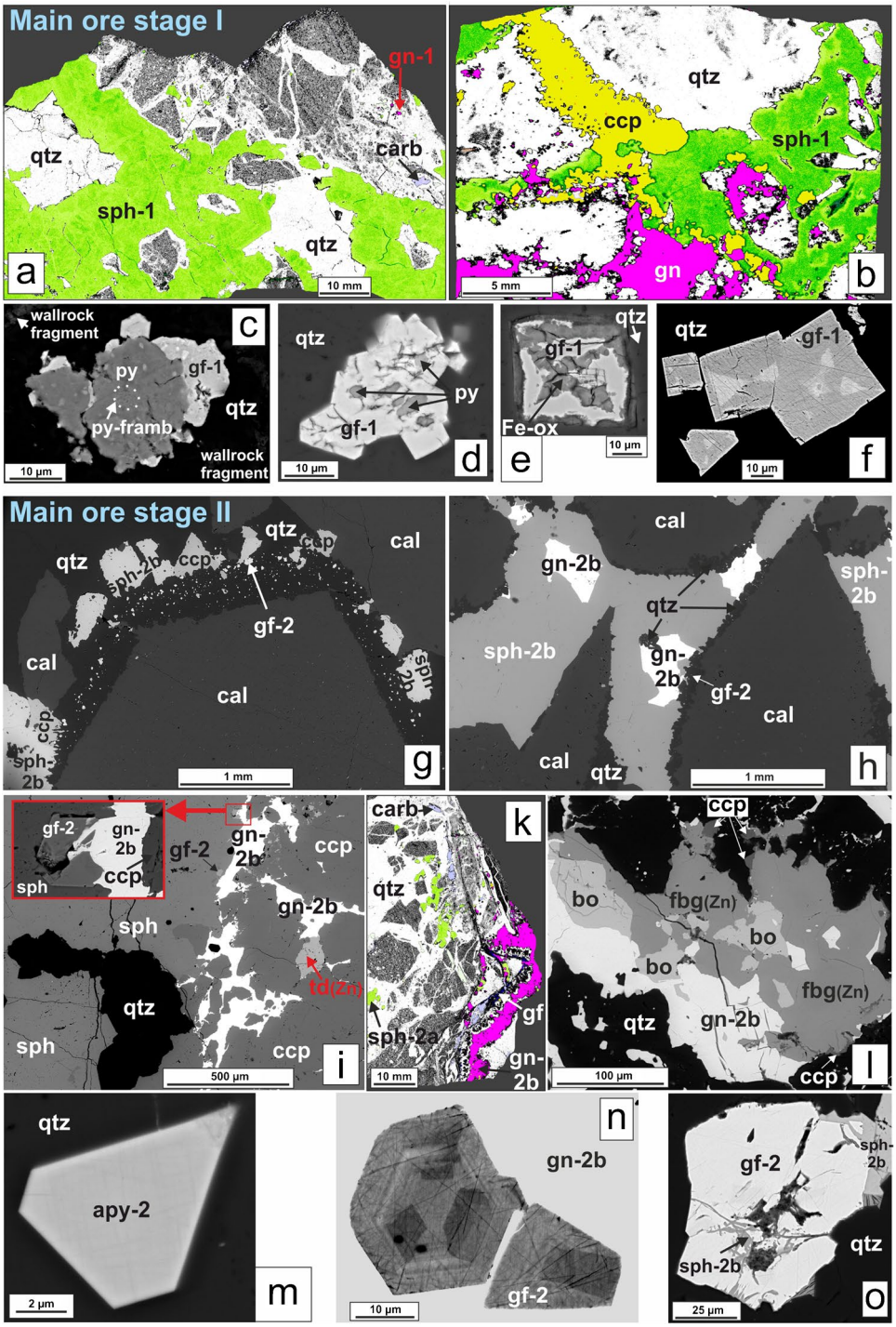

in Fig. 6(d)). The calcite shows $MgCO_3$ values between 0.15 and 0.42 wt% (mean, 0.22 wt%; $n = 17$; EPMA data of this study), which are similar to those for the identical ore stage (IIIa) at the Grund deposit (Sperling 1973). The $MnCO_3$ values are mainly between 1.70 and 3.26 wt% (mean, 2.51 wt%; $n = 17$). Calcite from the carbonate-sulfide stage at Lautenthal commonly hosts anhedral inclusions of siderite (up to 25 µm) and synchysite-(Ce-Nd) needles (up to ~ 80 µm in size; Table 1). Quartz forms thin overgrowths on rock fragments embedded in the calcite and on crystal faces of euhedral calcite. This quartz hosts gersdorffite-2, sphalerite-2b, chalcopyrite, and galena-2b (Fig. 5g, h). Fine grains (< 200 µm) of light-brownish sphalerite-3 of the post-ore stage are present in marcasite-3-(sphalerite-3)-calcite-quartz veinlets intersecting all older ore associations (Fig. 6(b); Table 2).

◂**Fig. 5** **a**–**o** Mineralogy of the Lautenthal (**a**–**d**, **f**–**i**, **m**, **o**) and the Bergstern veins (**e**, **k**–**l**, **n**) of the Lautenthal deposit. **a**, **b**, **k**. Color-coded mineral distribution maps (µ-EDXRF data). **c**–**i**, **l**–**o**. SEM-BSE images. **a**–**f**. Quartz-sulfide ore stage. **a** Sphalerite-1 with moderate Fe values (green) in breccia ore (BO; 500 m W). **b** Fe-richer sphalerite-1 (dark green) partly replaced by chalcopyrite (LO; Güte des Herrn mine; 8th mining level). **c** Pyrite-gersdorffite-1 aggregate from a brecciated vein segment (BO; 700 m W). An earlier core of framboidal pyrite is rimmed by coarser Fe sulfide (py) formed during the quartz-sulfide stage. Gersdorffite-1 forms an overgrowth on the Fe sulfide. **d** Gersdorffite-1 with pyrite inclusions from the marginal breccia of the vein (BO; 700 m W). **e** Gersdorffite-1 grain with altered pyrite remnants (BO; 330 m W). **f** Gersdorffite-1 with hourglass sector zoning (BO; 600 m W). **g**–**o** Carbonate-sulfide ore stage. **g**–**h** Euhedral calcite, overgrown by quartz hosting gersdorffite-2. The cavities between the carbonate are filled by sphalerite-2b, chalcopyrite, and galena-2b. **i**. Lens-shaped chalcopyrite-sphalerite-quartz aggregate, embedded in coarse-grained calcite (calcite not shown). The chalcopyrite is partly replaced by galena-2b and fahlore. Euhedral gersdorffite-2 is present at the interface between chalcopyrite/galena-2b and sphalerite (panels **g**–**i** from BO; 700 m W). **k** Vein breccia cut by a galena-2b-dominated veinlet, containing sphalerite-2b and gersdorffite-2. **l** Galena-2b-sulfosalt association. Freibergite-(Zn) replaces chalcopyrite and, subsequently, galena-2b replaces all older sulfides. Remnants of the chalcopyrite are present along the margins of the aggregate (panels **k**–**l** from BO; 370 m W). **m** Euhedral arsenopyrite-2 in quartz close to partly replaced sphalerite-1 (LO; Güte des Herrn mine; 8.th mining level). **n** Euhedral gersdorffite-2 with oscillatory growth zoning and sector zoning in galena-2b rich ore (BO; 370 m W). **o** Gersdorffite-2 fragments cemented by sphalerite-2b (BO; 700 m W). *apy*, arsenopyrite; *bo*, bournonite; *cal*, calcite; *carb*, carbonate; *ccp*, chalcopyrite; *fbg*, freibergite; *Fe-ox*, iron oxides; *gf*, gersdorffite; *gn*, galena; *py*, pyrite; *py-framb*, framboidal pyrite; *qtz*, quartz; *sph*, sphalerite; *td*, tetrahedrite. Orebodies: Bromberg (BO); Lautenthal (LO)

Minor and trace element distribution in sphalerite

Sphalerite is the main host mineral for high-tech trace metals in the Lautenthal veins. Laser ablation-ICP-MS minor and trace element data for sphalerite-1 and -2 of the main ore stages I and II are summarized in Table ESM 2 and plotted in Fig. 7. The much less abundant post-ore stage sphalerite-3 contains very low Fe (0.20 to 0.37 wt%; EPMA data) and its trace element content is extremely low (Table 2). Consequently, it is not further presented in this section.

Iron The Fe contents in sphalerite-1 and -2 are generally low to moderate and increase towards the eastern portion of the deposit (Fig. 7). In the Lautenthal orebody, sphalerite-1 with elevated Fe contents of up to 4.09 wt% (median values of eight samples, 1.95 to 3.22 wt%; Table ESM 2) was observed.

Cadmium This element shows a low variability in concentrations throughout the deposit. The Cd contents in sphalerite vary from 0.11 to 0.91 wt%, with median values ranging from 0.19 to 0.32 wt% for all locations (Table ESM 2). No differences are present between the orebodies and the ore stages. In the carbonate-sulfide stage, the distribution of Cd is, at least locally, crystallographically controlled (Fig. 8c). Here, zones with high Cd show moderate Fe, but are characterized by low contents in some trace elements (e.g., Cu, Sb, In, Ga; Fig. 8c–h).

Copper Its concentrations show a strong variation even on the grain scale. They commonly range from tens to a few thousands of ppm (Fig. 7). Two LA-ICP-MS measurement spots in samples from the Lautenthal vein (Kalkspatfirste) and the Bergstern vein (370 m West, Bromberg orebody) provided Cu values as high as 1.3 wt%. However, these spots occur close to chalcopyrite intergrown with or replacing sphalerite and the datasets may represent mixed analyses or submicron-sized inclusions. Sphalerite-1 shows two distinctly different patterns of Cu distribution. On the one hand, Cu-enriched patches or nests are linked to alteration-related textures in millimeter-scale remnant grains embedded in replacing chalcopyrite. These patterns were especially observed in moderately Fe-bearing sphalerite-1 of three samples from the Lautenthal orebody. On the other hand, sphalerite-1 not influenced by fluid-driven alteration commonly shows crystallographic control on the Cu distribution in the mineral (so-called sector zoning; cf. Johan 1988). The element distribution maps in carbonate-sulfide stage samples from the Bromberg orebody indicate that the distribution of Cu in sphalerite-2b is strictly crystallographically controlled. Its variation in concentration either outlines oscillatory growth zoning patterns or highlights sector zoning-related patterns (Fig. 8e). Copper enrichment in sphalerite-2b commonly follows Fe-depleted patterns in the mineral (Fig. 8d, e).

Antimony Its concentrations show a strong variation. Commonly, the Sb values range from some tens to a few hundreds of parts per million (Fig. 7). Maximum Sb concentrations of 0.2 to 0.3 wt% occur in sphalerite from most outcrops within the Bromberg orebody. Higher Sb concentrations are indicated for sphalerite-2b from the latter orebody (medians of samples, 115 to > 150 ppm), when compared to most sphalerite-1 (Fig. 7). All samples from the Lautenthal orebody, either overprinted by later fluids (cf. above paragraph focused on Cu) or largely unmodified, have Sb median/mean values in sphalerite-1 of less than ~ 65 ppm. A dependency of the Sb concentration in sphalerite on the depth level of the sampling positions in the vein system was not observed. Within grains, increased Sb concentrations commonly highlight sector zoning-related patterns (Fig. 8f). Such high-Sb patterns correlate with some of the high-Cu patterns; however, other Cu-rich patterns are low in Sb (red dashed circles in Fig. 8e, f).

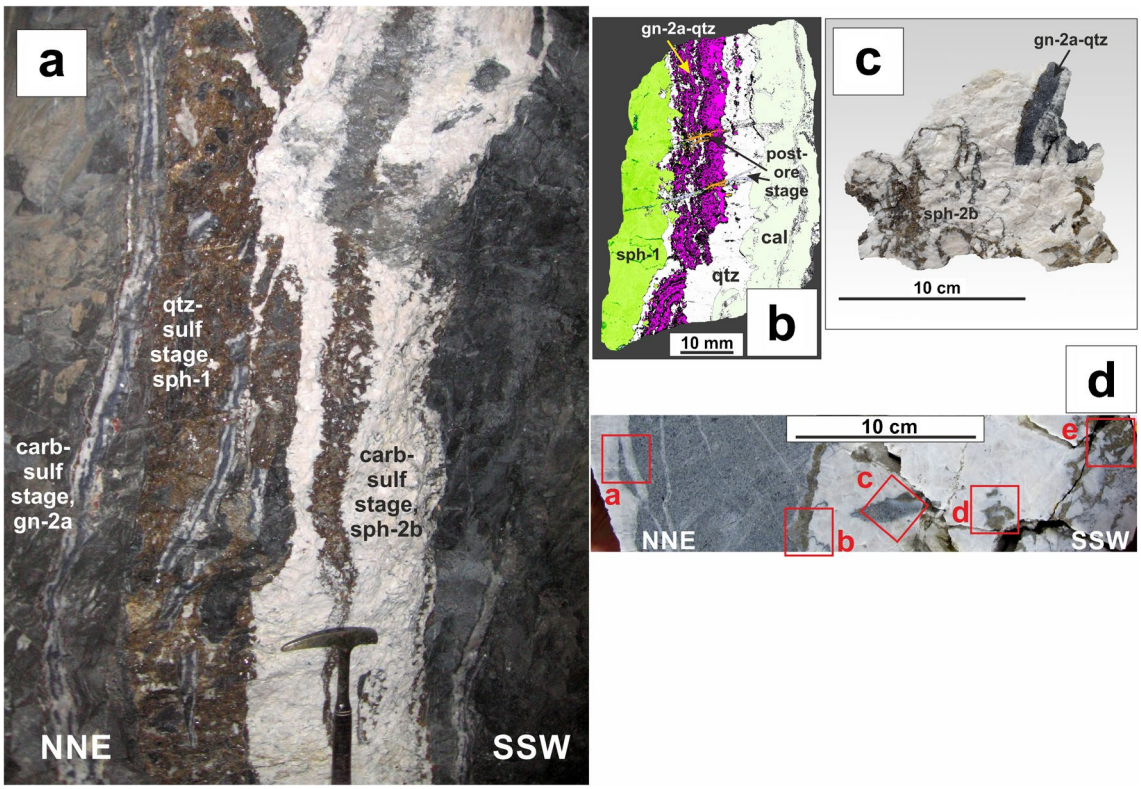

Fig. 6 Outcrop of base metal ores in the Lautenthal vein (central branch) showing the quartz-sulfide and carbonate-sulfide stages at crosscut 700 m West (Bromberg orebody). (**a**) Massive sphalerite-1 of the quartz-sulfide stage forms the NNE side of the ore, cut by several footwall quartz stringers containing galena-2a and subordinate sphalerite-2a of the quartz-dominated sub-stage of the carbonate-sulfide stage. The SSW side (central part) of the vein structure is formed by moderately sphalerite-2b-bearing ore of the carbonate-dominated sub-stage of the carbonate-sulfide stage. (**b**) Color-coded mineral distribution map for one of the footwall stringers (μ-EDXRF data). Green, purple, pale greenish, and white colors stand for sphalerite (sph), galena (gn), calcite (cal), and quartz (qtz), respectively, whereas orange colors stand for FeS_2. (**c**) Fragment of a footwall stringer (gn-2a-qtz; top right of specimen), which was tectonically rotated and, subsequently, embedded in calcite of the central part of the vein structure. (**d**) Profile covering the northern segment of the base-metal ore vein (margin to center). The large specimen containing this profile was taken from the roof of the crosscut. The profile was sampled (red squares) and the five sections (**a–e**) were studied here. For abbreviations of minerals see Fig. 5. Qtz-sulf stage, quartz-sulfide stage; carb-sulf stage, carbonate-sulfide stage

Tin Its concentrations are very low in most sphalerite grains. In many quartz-sulfide stage samples from both orebodies, less than 50% of the measurement spots yield measurable amounts of this trace element (Fig. 7). Somewhat elevated Sn concentrations were recorded for sphalerite-2b from the Bromberg orebody, with medians for sampling locations reaching values as high as 32 ppm (Bergstern vein). A final assignment of the variation of the Sn concentrations to zoning-related or other patterns in the carbonate-sulfide stage sphalerite is not possible at present. Overprinted sphalerite-1 from the Lautenthal orebody shows Sn enrichment when compared to unmodified sphalerite-1 (Fig. 7). In one sample from the Abendstern branch vein, Sn is concentrated in small, irregularly formed Sn-In-enriched domains in the mineral. Such domains were observed adjacent to the contact between sphalerite-1 and the replacing chalcopyrite. Very rare cassiterite grains (size 4 to 10 μm) occur in chalcopyrite aggregates of this sample (Weber 2013 and this study).

Silver The Ag median values for the samples range from 2 to 36 ppm (Table ESM 2). There are no significant differences in the Ag concentrations between the sample locations and ore stages (Fig. 7). Due to its overall low concentrations in sphalerite and the rather high background during EPMA element mapping, the distribution characteristics of Ag in sphalerite remain poorly constrained. However, moderate enrichment of Ag in sector zoning-related patterns showing also Cu and Sb enrichment is indicated for at least one carbonate-sulfide stage sphalerite sample by EPMA-WDS element mapping.

Germanium The element is uniformly incorporated into the lattice of sphalerite from both sulfide ore stages in rather low concentrations, with maximum values ranging from 55 to ~ 210 ppm for individual samples (Fig. 7). Median values for Ge range from ~ 1 to 11 ppm for both orebodies (Table ESM 2).

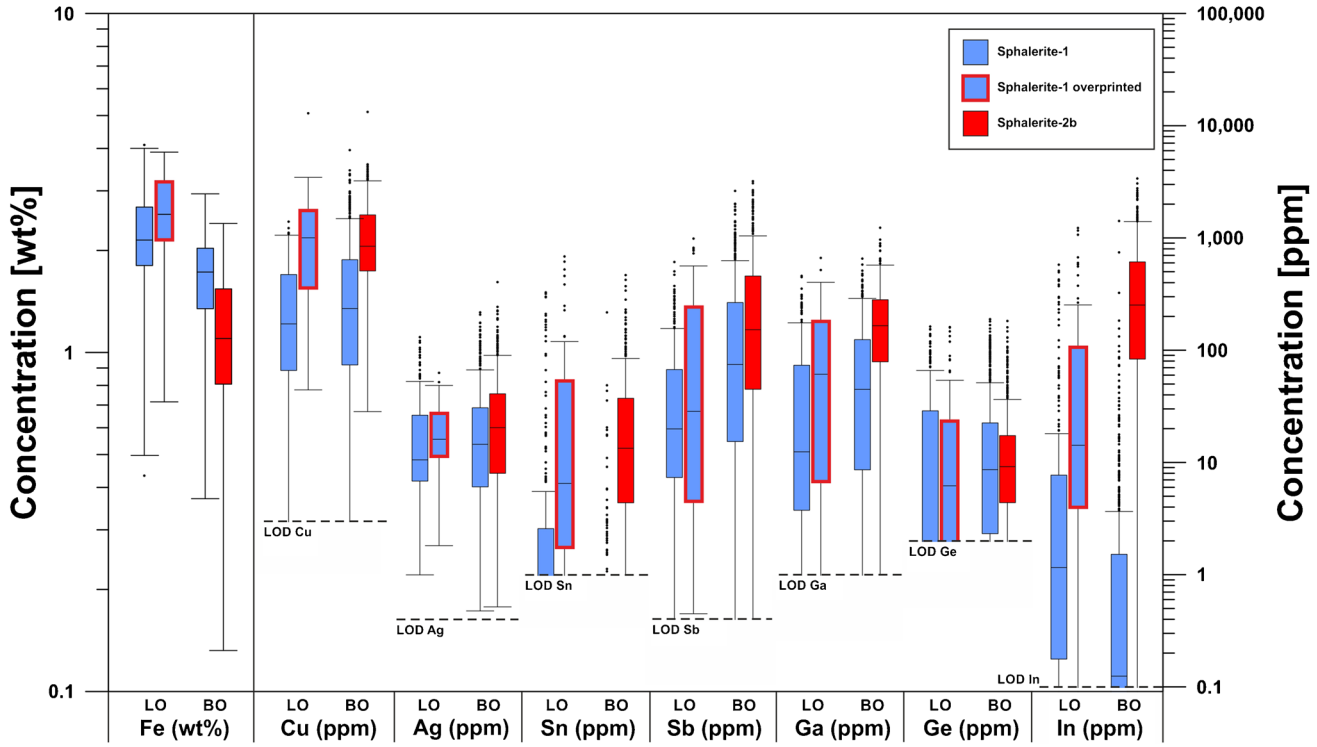

Fig. 7 Box plot diagrams for Fe, Cu, Ag, Sn, Sb, Ga, Ge, and In in sphalerite-1 of the quartz-sulfide stage from the Lautenthal orebody (blue boxes (LO); 230 laser spots in 4 samples) and the Bromberg orebody (blue boxes (BO); 517 spots in 12 samples) as well as in later overprinted sphalerite-1 from the Lautenthal orebody (blue boxes with red outline (LO); 71 spots in 3 samples) and sphalerite-2b of the carbonate-sulfide stage from the Bromberg orebody (red boxes (BO); 429 spots in 12 samples). Median values, whiskers (1.5 times the interquartile range), outliers, and mean limits of detection (LOD) of LA-ICP-MS datasets are shown in the plots

Indium Its concentrations show the highest variability of all trace elements in sphalerite from Lautenthal (Fig. 7). This observation applies for the macroscopic scale (i.e., the position of a sample in the vein system and its assignment to an ore stage), and also for the individual sphalerite grain scale. The lowest In values in the sphalerite lattice were recorded for all quartz-sulfide stage samples from both orebodies that show no indication for significant sphalerite-1 replacement by chalcopyrite (Fig. 7). Especially low In concentrations occur in the sphalerite-1 from the brecciated Lautenthal vein at crosscut 500 West (Bromberg orebody). Here, > 50% of the spot measurements were below the LOD of the LA-ICP-MS method for In. Partly replaced and altered sphalerite-1 grains of the Lautenthal orebody show moderately enriched In concentrations (median/mean for samples ~ 11 to ~ 80 ppm In), when compared to "normal" sphalerite-1 (Fig. 7). Indium-enriched domains in these grains are clearly linked to alteration-related textures (e.g., patches, nests, domains arranged adjacent to cracks or cleavage planes). However, the highest In concentrations at Lautenthal occur in sphalerite-2b from the Bromberg orebody (Fig. 7), with a maximum concentration of 0.34 wt% for an individual measurement spot (Bergstern vein). The median values for carbonate-sulfide stage vein outcrops within the Bromberg orebody range from ~ 5 to 574 ppm (sphalerites-2a and -2b; Table ESM 2). The distribution of In in carbonate-sulfide stage sphalerite is strongly crystallographically controlled. The variations in concentration often highlight sector zoning-related patterns of the mineral and, less commonly, outline narrow oscillatory growth zoning patterns. Clearly visible in the element distribution maps is the spatial correlation of In-rich with some Cu-rich patterns (Fig. 8e, g). However, a striking feature is the divergent (mutually exclusive) arrangement of In-rich and Sb-rich patterns in the crystal structure of sphalerite (red dashed circles in Fig. 8f, g). However, both patterns combined fit well with zones of Cu enrichment (circles 1–3 and 5 in Fig. 8e–g).

Gallium Its concentrations in sphalerite have median values for the individual vein outcrops of both ore stages and in both orebodies between 6 and 165 ppm (Table ESM 2). A difference in concentrations between "normal" and overprinted sphalerite-1, as observed for a number of other trace elements, might be present also for Ga (Fig. 7). Sphalerite-2b from the Bromberg orebody shows the highest median Ga concentrations within the Lautenthal deposit (153 to 165 ppm). Gallium incorporation into the sphalerite-2b lattice is crystallographically

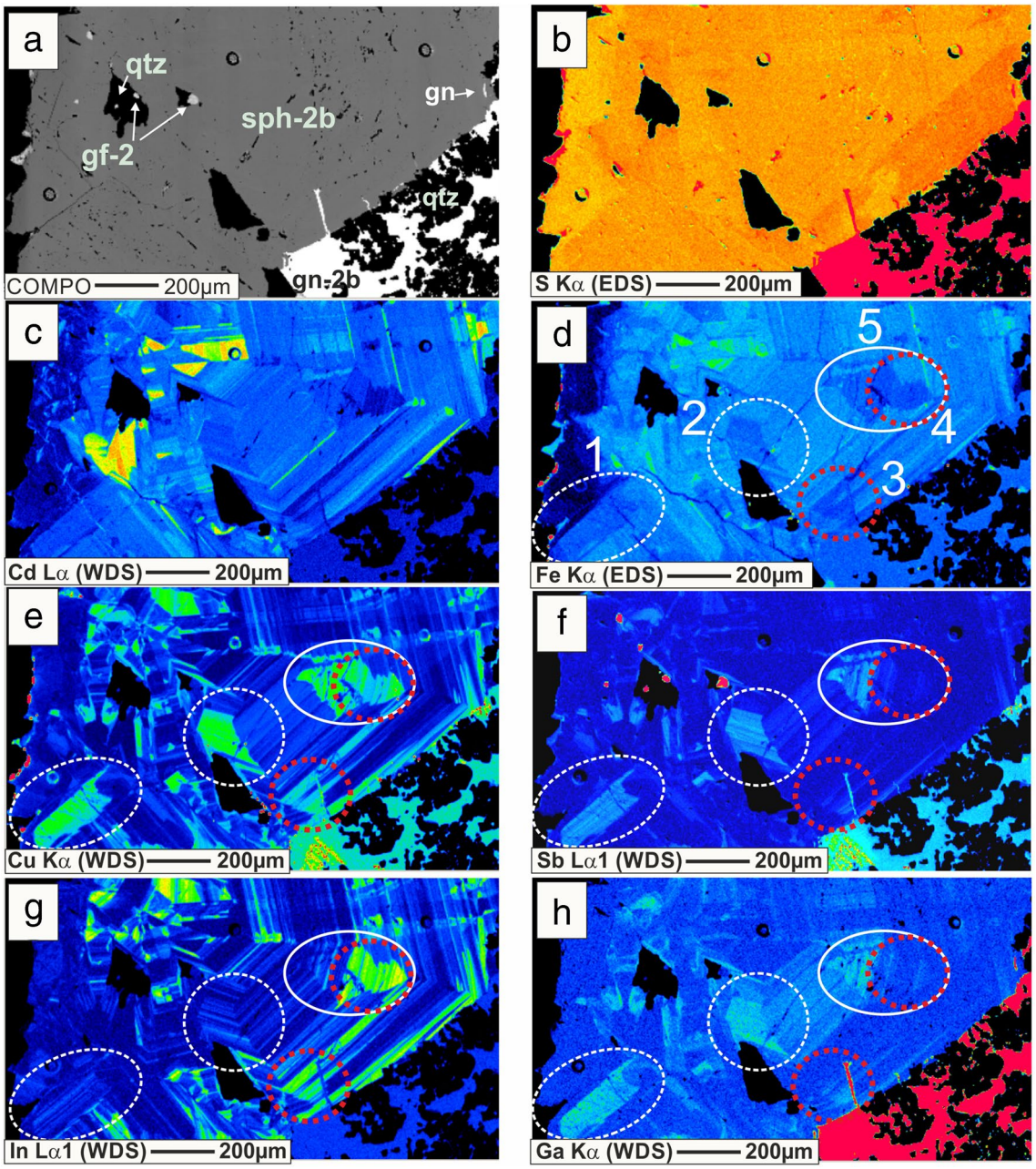

Fig. 8 **a**–**h** Semi-quantitative element distribution maps for major, minor, and trace elements in sphalerite-2b from the carbonate-sulfide stage of the Bergstern vein (370 m West; Bromberg orebody). All data were determined using EPMA (WDS or EDS methods). Dashed circles 1 to 4 in figures d to h highlight crystallographic zones in the mineral grain with contrasting behavior of trace element incorporation: 1 and 2 (white)—low Fe, high Cu, high Sb, low In, high Ga; 3 and 4 (red)—low Fe, high Cu, low Sb, high In, low Ga. For abbreviations of minerals see Fig. 5

controlled and follows the sector zoning-related patterns as highlighted by Fe depletion and Cu enrichment (Fig. 8d, e, h). A sample from Maassen mine hosts two sphalerite generations (Weber 2013); the older Fe-richer sphalerite is Ga-rich (Fe, 1.7 wt%; Ga, 188 to 193 ppm), whereas the younger one (probably sphalerite-3) is Ga-poor (Fe, 0.3 wt%; Ga, 7 to 10 ppm).

Trace element concentrations in hand-picked sphalerite samples and ore concentrates

To evaluate and scale-up the micro-analytical data, sphalerite from both main ore stages within the Lautenthal vein was concentrated in hand-picked samples and ore concentrates.

The In concentrations and In/Zn values in the hand-picked sphalerite samples from the Bromberg orebody show a steady increase from 500 m West and 600 m West, over the footwall branch vein at 700 m West, to the central branch vein at 700 m West (Table 3). The Cu values are almost identical for the first three locations and are higher for the central branch samples. Gallium and Sn show similar trends. Despite the fact that the first three locations host sphalerite-1-dominated ore of the quartz-sulfide stage only, there is a difference in In concentrations between them (Table 3). The high In and moderate Sn values in the samples from the central branch of the vein at 700 m West indicate a high In level and associated moderate Sn enrichment in the sphalerite-2a and -2b ore of the carbonate-sulfide stage at this location. Thus, these bulk data confirm the EPMA and LA-ICP-MS micro-analytical data for the respective sphalerite generations.

Both sphalerite-1-enriched moderate volume ore concentrates from 500 m West are similar in base metal and trace element (Cu, Ga) compositions. Indium and Sn concentrations are below the LOD of the method (1 sample; Table 3). Moderate volume concentrates from both locations at 700 m West confirm the trace element compositional trend observed for the respective hand-picked samples. Despite rather low Zn contents in the carbonate-sulfide stage-dominated ore from the central branch vein, weak Sn and strong In enrichment (up to ~ 109 ppm) is indicated here, when compared to the quartz-sulfide stage ore of the footwall branch vein (Table 3). Finally, the 700 m West sample composed of > 50 kg of mixed ore from both main ore stages (A. Haas, pers. comm.) still contained significant In concentrations (82 ppm; In/Zn, 0.44×10^{-3}) despite low Zn contents in the ore (Haas 2020).

The historical industrial mixed ore concentrate from the Lautenthal orebody sampled during ore processing in 1922 probably contains sphalerite of all generations. However, its In concentration and In/Zn value are in the same order of magnitude like those data for the mixed ore concentrate from 700 m West (Table 3).

Mineral geothermometers

Gersdorffite-1 neither displays significant substitution of As for S (As:S atomic ratio, 0.89 to 1.08(1.15); median, 0.96; $n = 98$), nor significant substitution of Sb for As (Sb:As atomic ratio, < 0.001 to 0.057; median, 0.003; $n = 98$). Therefore, its chemical data can be plotted in the NiAsS-CoAsS-FeAsS diagram (Fig. 9) as constructed by Klemm (1965), which shows the stability fields of solid solutions dependent on the temperature of synthesis. The plotted positions of the gersdorffite-1 data (Bromberg orebody) in the diagram allow to estimate temperatures of precipitation for the mineral at about 300 °C or slightly below 300 °C. On the other hand, significant substitution of Sb for As is indicated for a large portion of the gersdorffite-2 grains and consequently their mineral chemistry data cannot be used for a temperature estimation. Klemm (1965) assumes a large uncertainty of the NiAsS-CoAsS-FeAsS temperature estimation below 300 °C; no specific values are provided.

Using the sphalerite geothermometer GGIMFis (Frenzel et al. 2016), median crystallization temperatures of the sphalerite-1 were calculated between 151 and 204 °C for LA-ICP-MS data of 12 samples (Table ESM 2; Table 3) from the Bromberg orebody (median for all samples, 174 °C). In the Lautenthal orebody, the calculated median values for sphalerite-1 samples are between 198 and 246 °C (median for all samples, 230 °C). GGIMFis temperatures for overprinted sphalerite-1 do not differ substantially from those for unmodified sphalerite-1 (Table ESM 2). Crystallization temperatures of the carbonate-sulfide stage sphalerite-2 were calculated between 158 and 210 °C for LA-ICP-MS data of 13 samples from the Bromberg orebody (median for all samples, 184 °C; Table 3). The uncertainty of the GGIMFis temperature estimation in the temperature range relevant for Lautenthal is ± 60 °C (Frenzel et al. 2016).

Discussion

The data indicate that Ga and locally In show the highest enrichment among the high tech-relevant trace elements and are predominantly hosted by sphalerite in the Lautenthal base metal veins. Tin concentration is low. Discrete In-bearing minerals like roquesite ($CuInS_2$), sakuraiite ((Cu, Zn, Fe, In, Sn)S) or dzhalindite ($In(OH)_3$), which commonly occur in In-rich epithermal deposits (e.g., Cook et al. 2009), were not observed in the Lautenthal veins.

From the evaluation of the ore concentrate data, it is inferred that the In-bearing ore type at Lautenthal, as for example represented by the complex carbonate-sulfide ore outcrop at crosscut 700 m West (Fig. 6(a)), contains Zn ore with average In contents up to > 100 ppm. Thus, In enrichment at Lautenthal locally may reach economically relevant concentrations.

The first part of the discussion focuses on an interpretation of the observed high tech-element distribution in sphalerite. Finally, the sphalerite mineral chemistry data are comparatively discussed with adjacent hydrothermal systems from the Upper Harz and worldwide equivalents.

Interpretation of trace element distribution in sphalerite: incorporation mechanisms

Divalent cations (e.g., Fe, Cd) show a strong negative correlation with Zn in our sphalerite dataset and substitute directly for Zn^{2+} cations into the sphalerite lattice. In

Table 3 Chemical composition (base metals and selected trace metals) of sphalerite samples from outcrops of the Lautenthal vein as determined using ICP-OES and ICP-MS

Location	Bromberg orebody; crosscut 500 m West					Bromberg orebody; crosscut 600 m West	Bromberg orebody; crosscut 700 m West, footwall branch			Bromberg orebody; crosscut 700 m West, central branch			Bromberg orebody; crosscut 700 m West	Lautenthal orebody; Güte des Herrn mine
Ore stage	Quartz-sulfide					Quartz-sulfide	Quartz-sulfide			Quartz-sulfide/carbonate-sulfide			Quartz-sulfide/carbonate-sulfide	Unknown
Dominant sphalerite generation	1					1	1			2/(1)			2/1	Unknown
Sample type	Hand-picked sphalerite sample[a]			Moderate volume concentrate[b]	Moderate volume concentrate[b],*	Hand-picked sphalerite sample[a]	Hand-picked sphalerite sample[a]		Moderate volume concentrate[b]	Hand-picked sphalerite sample[a]		Moderate volume concentrate[b]	Moderate volume concentrate[b],*,**	Industrial ore concentrate[c]
Zn (wt%)	47.9	48.8	64.4	20.9	24.6	43.0	63.0	63.0	46.7–51.9	52.9	55.0	27.0–27.7	18.8	8.1
Pb (wt%)	0.02	0.01	0.13	2.23	3.30	1.08	0.1	0.06	0.15–0.24	1.16	0.36	0.07–1.39	0.75	8.3
Fe (wt%)	1.42	1.54	1.63	0.90	0.97	1.77	1.01	1.04	0.78	1.07	1.10	0.79–0.92	1.03	8.3
Mn (ppm)	81.0	108	71	n.a	n.a	773	196	185	n.a	470	318	n.a	n.a	5791
Cu (ppm)	430	450	750	261	309	650	580	580	404–429	1430	1540	343–490	516	39,500
Ga (ppm)	108	107	124	29.7	41	41.0	125	124	76.5–84.0	143	150	54.0–59.7	65	28
Ge (ppm)	40.0	39.8	40.0	21.3	n.a	3.70	22.4	21.9	8.50–13.0	17.7	20.0	< 2	n.a	< 1
In (ppm)	< 0.2	0.20	< 0.7	< 2	n.a	1.10	26.1	29.6	8.07–8.84	378	375	66.4–109	82	37.7
Sn (ppm)	< 0.5	< 0.5	22.5	< 4	n.a	0.60	1.60	1.60	< 2	19.6	19.9	4.32–5.34	n.a	16.0
1000 In/Zn		0.0004				0.003	0.04	0.04	0.02	0.71	0.68	0.25–0.39	0.44	0.46
GGIMFis temperatures calculated using LA-ICP-MS data; median for all samples (°C; ± 60 °C)***	174					179	166			184				230

n.a. not analyzed

[a]Sample weight: 48 to 71 g

[b]Sample weight: 0.5 to > 50 kg

[c]Historic industrial mixed-ore concentrate from the Güte des Herrn mine (13th Feldortstreckenfirste; concentrate dated 1922)—data source: Graupner et al. (2019)

*Data source: Haas (2020)

**The concentrate may contain material from both studied ore zones at 700 m West (A. Haas, pers. comm.)

***For details, see text; data for individual samples are part of Table ESM 2; values below LOD were set to 50% of LOD for calculation of GGIMFis temperatures

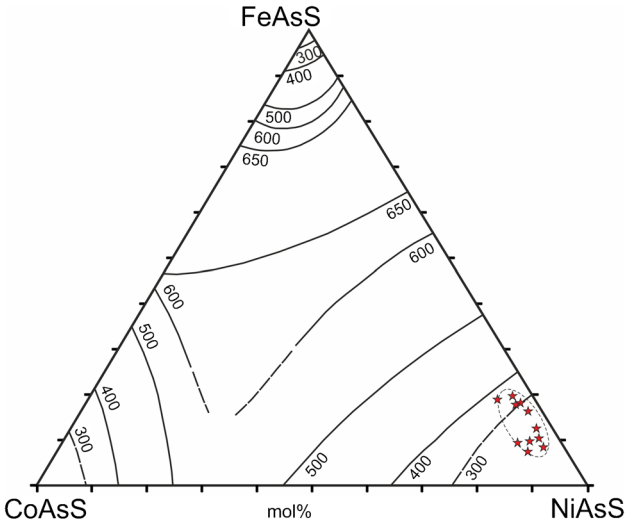

Fig. 9 Compositional plot of the gersdorffite-1 from the Bromberg orebody in the system NiAsS-CoAsS-FeAsS. Each red star in the diagram stands for the average composition of the gersdorffite-1 in one individual sample. Solvus lines at different temperatures (in °C) are taken from Klemm (1965)

contrast, the trivalent cations (e.g., Sb, Ga, In) substitute for Zn in the sphalerite structure by coupled substitution mechanisms involving monovalent cations (e.g., Ag, Cu) or by resulting vacancies (cf. Cook et al. 2009). The positive correlation of Sb^{3+} and Cu^{+} (LA-ICP-MS data; see ESM; Fig. ESM 1a) in the In-bearing samples of the calcite-dominated sub-stage of the carbonate-sulfide stage from the Bergstern and Lautenthal veins supports their crystallographically controlled incorporation as indicated by EPMA element mapping (Fig. 8e, f). The presence of data points below the 1:1 line in the Sb^{3+} versus Cu^{+} plot indicates the involvement of other trivalent cations. Monovalent Ag shows a strong positive correlation with Sb above the 1:1 line (Fig. ESM 1b). The cations Ga^{3+} (Fig. ESM 1d) and In^{3+} do not show a clear correlation trend with monovalent Ag. However, a positive correlation with Cu^{+} is indicated for both elements (Figs. ESM 1c,e), supporting the results of EPMA element maps (Fig. 8e, g, h). In general, the presence of monovalent cations enabled the incorporation of Sb, In, and Ga into the sphalerite lattice in the investigated samples by coupled substitution (Fig. ESM 1f), but low concentrations of other cations or the formation of vacancies may have contributed to the incorporation of the above elements as well. Possible incorporation mechanisms of Sb, In, and Ga into In-bearing sphalerite of the Bergstern and Lautenthal veins are shown in the following equations (cf. Sahlström et al. 2017; Henning et al. 2022):

$$2Zn^{2+} \leftrightarrow (Sb, In, Ga)^{3+} + (Cu, Ag)^{+} \quad (1)$$

$$3Zn^{2+} \leftrightarrow 2Ga^{3+} + \square \quad (2)$$

It is very likely that the oscillatory or zone-controlled incorporation of Cu + In + (Sb) represents the result of fluctuation in temperature during sphalerite precipitation. However, elevated concentrations of Cu, Ag, and Sb may also hint towards the presence of nano-scale mineral inclusions (e.g., tetrahedrite or freibergite) in the sphalerite. Copper (and some of the other mentioned elements) may have formed nanocrystals of Cu-Sb sulfides that cluster especially into sector zones. Antimony is commonly not present in solid solution in sphalerite at elevated concentrations. But, coupled substitution allows the incorporation of Cu into the sphalerite structure in In-bearing samples without chalcopyrite disease (Cook et al. 2009). Therefore, the strong crystallographic control (Fig. 8) and the absence of chalcopyrite disease may indicate the incorporation of these elements into the sphalerite structure in our dataset. A proper statistical analysis on Sn and Ge behavior is not possible due to their presence in elevated concentrations (> 50 ppm) in only < 10 and < 15% of the laser spots, respectively. Although EPMA—having smaller spot sizes than LA-ICP-MS—did not confirm a frequent presence of micro-inclusions of Cu-Ag-Sb or Sn minerals (e.g., cassiterite), their occurrence as tiny interstitial inclusions in certain domains of the sphalerite at Lautenthal cannot be excluded.

Lateral main ore stage I geochemical zonation: constraints from mineral geochemistry and geothermometers

Mineralogical data for the quartz-sulfide stage show substantial variation throughout the Lautenthal deposit. Most evident is the irregular but clearly visible increase in Fe concentrations for sphalerite-1 from the Bromberg orebody towards the easternmost segments of the vein system in the Lautenthal orebody. Median In and Sn values are at very low levels, with Sn always close to or below the LOD of the LA-ICP-MS. However, In and Sn seem to be somewhat more frequent in sphalerite-1 from the Lautenthal orebody compared to the Bromberg orebody. The other trace elements measured in sphalerite-1 behave inconsistently (Fig. 7). Whereas median Cu and Ag concentrations are similar for samples from both orebodies, median Sb, Ga, and Ge values are higher for the Bromberg orebody. Whether these chemical variations reflect lateral geochemical zonation for main ore stage I along the Lautenthal fault zone remains open. Frenzel et al. (2016) states that Fe and In are on the high-temperature calibration side of the GGIMFis thermometer, whereas Ga and Ge decrease with increasing formation temperatures of sphalerite. This explains the GGIMFis

crystallization temperature estimates for Lautenthal (Table ESM 2), which are constantly higher for sphalerite-1 from the Lautenthal orebody (median, 230 °C) compared to sphalerite-1 from the Bromberg one (median, 174 °C), allowing to take a lateral temperature zonation within the hydrothermal system into consideration. Figure 4b illustrates that both orebodies differ regarding their depth extensions and, consequently, the calculated GGIMFis temperature difference may reflect different exhumation levels for them. Observed higher frequencies of occurrence of gersdorffite-1 and the presence of larger crystal sizes of them in the Bromberg compared to the Lautenthal orebody provide another argument for the above assumption. The rather large uncertainties of the gersdorffite and GGIMFis temperature estimations in the temperature range relevant for the quartz-sulfide stage at Lautenthal allow no detailed statement about a temperature evolution from initial to later parts of this stage. However, the gersdorffite-1 data provide a temperature estimate for the initial part of this stage with ~ 300 °C (or slightly lower; Fig. 9), which probably characterizes the maximum temperature conditions for the assumed ascending metal-bearing brines. The formation of banded base metal sulfide ores of the Upper Harz district is commonly explained by mixing of such brines with lower-temperature, H_2S-bearing fluids at the depositional site (e.g., Möller et al. 1984; Lüders and Ebneth 1993). Such a fluid mixing prior to sphalerite formation could explain the reduced GGIMFis temperature estimates for the moderate Fe- and low In-bearing sphalerite-1 at Lautenthal (Table 3; Table ESM 2). GGIMFis temperature estimates for sphalerites of the quartz-sulfide and the carbonate-sulfide ore stages of the respective orebodies overlap within the uncertainty of the method. Fluctuations in the fluid temperature are indicated by zone-controlled trace element patterns in sphalerite. Fluid temperature estimates from fluid inclusion data are not available for Lautenthal.

Indium-enrichment process during main ore stage II and comparison of both ore stages

Reactivation of fault structures during the carbonate-sulfide stage allowed precipitation of moderate volumes of base-metal sulfides. Hydrothermal fluid circulation during this stage affected sphalerite-1-bearing vein assemblages and triggered local sphalerite-1 replacement by chalcopyrite (Fig. 5b). However, all chalcopyrite at Lautenthal has similarly low In concentrations (max., ~ 11 ppm In; $n = 150$; LA-ICP-MS data of this study) like the "unmodified" sphalerite-1 from both orebodies (Fig. 7). A genetic link of both (i) secondary In enrichment in sphalerite-1 domains that are partly replaced by chalcopyrite of the carbonate-sulfide stage, and (ii) primary In incorporation in sphalerite-2b (Fig. 7) due to a probably Cu-In-bearing fluid, is likely. It is assumed that chalcopyrite overgrowing and replacing sphalerite-1 consumes S during its precipitation, which is provided by the dissolution of the sphalerite-1. Consequently, the fluid becomes increasingly enriched in Zn, which in turn facilitates the redistribution of Zn over a short distance. The evolution of the hydrothermal fluid was controlled by its primary composition and by interaction with the pre-existing solid mineral phases of the veins. Saturation of Zn in the fluid results in the precipitation of texturally younger sphalerite-2. As the crystallographically controlled In patterns in sphalerite-2b are correlating with Cu-rich patterns and this sphalerite occurs associated with gersdorffite-2, it is assumed that a Cu-Sb-In-bearing fluid of the carbonate-sulfide stage supplied In and replaced In-poor sphalerite-1.

Besides the ore textures, a substantial difference between the main ore stages at Lautenthal concerns the minor element compositions of the accessory Fe-Co-Ni sulfarsenides (mainly gersdorffite). Furthermore, main ore stage II contains slightly higher contents in Cu-Sb minerals than stage I, and higher concentrations of In are present in sphalerite-2 compared to those in sphalerite-1. A combination of these distinguishing features between the stages is used to put further constraints on the processes resulting in formation of the carbonate-sulfide stage. The trace element characteristics of Fe-Co–Ni sulfarsenide–sphalerite pairs of minerals, representing each individual ore stage, are plotted in Fig. 10. Both minerals always occur in direct spatial association within studied samples. For the Sb concentration in Fe-Co-Ni sulfarsenide grains, the median and maximum values of each sample are given, whereas the In concentrations in sphalerite grains are represented by the median values of the respective sample ($n = 25$). The sample origin for each Fe-Co-Ni sulfarsenide–sphalerite pair is listed in the legend of Fig. 10 for both orebodies.

In Fig. 10, quartz-sulfide stage ore constantly plots at low Sb and In values. However, the Sb concentrations in gersdorffite-1 from the Lautenthal orebody seem to be even lower than those in gersdorffite-1 from the Bromberg orebody. Constantly high Sb and In concentrations for the two minerals characterize all samples from the carbonate-sulfide stage ore within the Bromberg orebody. However, the data suggest a linear trend between these two extreme fields with a slight offset between the two orebodies. The differences between points with similar In on both trend lines (left trend line in the figure: Lautenthal orebody; right trend line: Bromberg orebody) are ascribed to the Sb concentrations in gersdorffite. The trend is interpreted to indicate variable degrees of overprinting of older quartz-sulfide stage ore and/or variations in fluid compositions in structures located in the surroundings of vein structures that were intensely reactivated during the carbonate-sulfide stage.

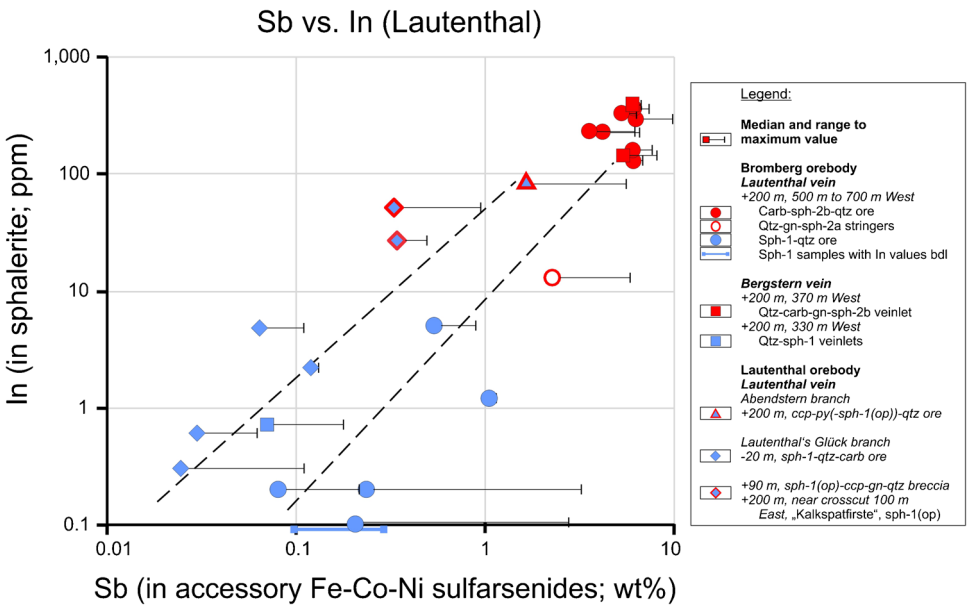

Fig. 10 Plot of Sb concentration in accessory Fe-Co-Ni sulfarsenides versus In concentration in sphalerite for Lautenthal base metal vein samples. The sulfarsenides (mainly gersdorffite) and sphalerite grains of each combined dataset (pair of minerals) always derive from identical ore stage, position in the respective mineralization, and, importantly, from an identical sample. Several sphalerite samples of the quartz-sulfide stage constantly yielded very low In concentrations with resulting median values below the LOD of the LA-ICP-MS method. To show the approximate position of the data for these samples in the plot, a Sb range for some samples is indicated outside of the diagram field by a thick blue line connecting median Sb values of samples. The two trend lines added in the figure connect the two "fields" for both stages for the Bromberg and the Lautenthal orebodies, respectively; see text for details. For abbreviations of minerals see Fig. 5. *Sph-1(op)*, sphalerite-1 overprinted by later stage fluids (blue symbols with red outline)

Furthermore, chalcopyrite attributed to the carbonate-sulfide stage shows replacement by tetrahedrite-(Zn) or freibergite-(Zn) (Fig. 5i, l; Table 2). If S is treated as the only relatively immobile element in the latter replacement/precipitation processes (cf. Wagner and Cook 1997), an influx of Cu, Ag, Zn, and Sb can be assumed. The dissolution of the sphalerite-1 provided the source of Zn, whereas Cu, Ag, and Sb must have been present in the mineralizing fluids of the carbonate-sulfide stage at significant concentrations. Mineral associations of chalcopyrite and fahlore-(Zn) that commonly occur nearby to both In-enriched modified sphalerite-1 and high-In sphalerite-2b (e.g., Lautenthal and Bergstern veins) suggest that the fluid active during the carbonate-sulfide stage is represented by a Cu-Sb-Ag-In-bearing fluid. Slight In enrichment in quartz-sulfide stage ore from the footwall branch at crosscut 700 m West (Table 3) supports the above assumption that carbonate-sulfide stage fluid circulation affected adjacent older vein structures. Furthermore, the Fe content in sphalerite-1 was probably too low to initiate significant diffusion of Cu into the sphalerite to produce chalcopyrite disease (cf. Bente and Doering 1993; Lepetit et al. 2003).

Indium-bearing ore associations in adjacent hydrothermal systems of the Upper Harz Mountains

Despite the fact that the Middle Devonian stratiform Pb-Zn-Cu deposit Rammelsberg, ~ 10 km NE of Lautenthal (Fig. 2), is older than the Pb–Zn-mineralized vein systems in the Upper Harz, it is worth to mention that this deposit hosted large volumes of In-enriched ore (mixed ore: In ≤ 77 ppm, Sn 50 ppm; Cu-rich ore: In 40 ppm, Sn ~ 300 ppm; e.g., Kraume 1955; Brauer 2013).

Considering base metal ore-bearing vein-type deposits in the study area, variable In concentrations are found in late, slightly Fe-enriched sphalerite (up to ~ 6 wt% Fe) from the hydrothermal vein deposit at Großfürstin Alexandra (GFA) mine (Graupner et al. 2019), located ~ 8 km NE of Lautenthal (Sperling and Berthold 1979; Stedingk 1982; Fig. 2). Median In values for three sphalerite samples range from 2 to ~ 120 ppm, with a maximum In concentration of ~ 700 ppm. The median for Sn in two sphalerite samples is 39 ppm (LA-ICP-MS data) and in the third sample 300 ppm (EPMA

data; Fig. 11; Graupner et al. 2019). The sulfide ores of the Lautenthal and the GFA mines are similar in some respects. This includes a Zn dominance of the ore at both locations, similar Sb concentrations and Ag contents of the Pb ores, with the latter being rather low relative to other Pb ores from the Upper Harz Mountains (Ahrend and Seidensticker in Kraume 1964). However, the common occurrence of oriented chalcopyrite and/or pyrrhotite micro-inclusions in anhedral sphalerite in the GFA veins (Stedingk 1982; Hall 2019) is different compared to their scarcity in sphalerite at Lautenthal.

For the world-class hydrothermal vein deposit Grund (~8 km S of Lautenthal; Fig. 1), which is paragenetically similar to Lautenthal (e.g., Sperling and Stoppel 1979), 18 sphalerite ore samples from the West Field orebody were measured for trace elements (Gundlach (1958) in Sperling 1973). The sphalerite contains between 10 and 140 ppm In (median, 30 ppm), 20 to 100 ppm Ga (median, 50 ppm), and 10 to 280 ppm Sn (median, 89 ppm). Sphalerite from drill core partly intersecting unmined portions of various depth levels of the West Field orebody II contains < 1 to 116 ppm In, 22 to 147 ppm Ga, and 1 to 220 ppm Sn, with median values of 12 ppm In, 75 ppm Ga, and 17 ppm Sn (ICP-MS data; $n = 141$; Stedingk 1993: Fig. 11). Iron contents in sphalerite from this orebody reach up to 8 wt% and its central segment often shows Fe (max) values > 5 wt% (Sperling 1979). Industrial sphalerite concentrates and one moderate volume sphalerite concentrate contain between 6 and 22 ppm In, 73 and 86 ppm Ga, and 12 and 111 ppm Sn (ICP-MS data; Graupner et al. 2019; Fig. 11). Oriented micro-inclusions do not occur in sphalerite from this deposit.

Sediment-hosted hydrothermal Zn-Fe-Pb mineralized zones from the Lower Saxony Basin to the NW of the Upper Harz are characterized by overall low minor and trace element contents in the sphalerite (median values for Ga and In are 0.99 ppm and 0.064 ppm, respectively; Nadoll et al. 2019) in contrast to studied locations in the Upper Harz.

Comparison of Lautenthal with magmatic-hydrothermal, vein-style Sn-In-rich systems worldwide

Vein-style In-rich ore formed at high (> 300 °C) or more moderate (~ 300 to < 300 °C) temperatures (Seifert and Sandmann 2006; Dill et al. 2013; Jovic et al. 2015), and is commonly attributed to tin-polymetallic veins and epithermal ore systems (Cook et al. 2009; Dill et al. 2013; Murakami and Ishihara 2013; Jovic et al. 2015). The deposits are spatially and temporally related to mainly subvolcanic rocks and represent magmatic-hydrothermal systems. They are characterized by high Sn concentrations in

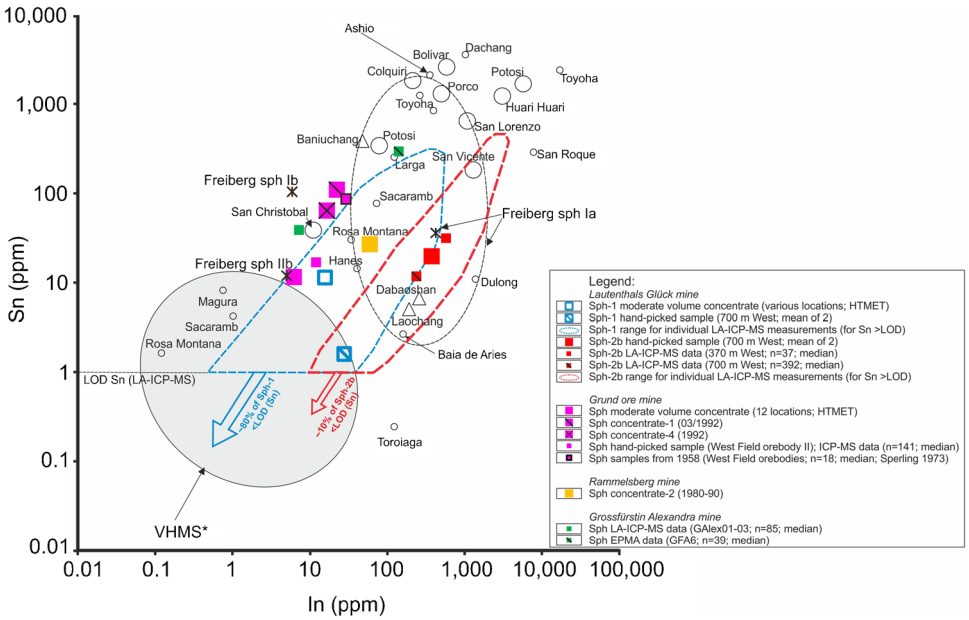

Fig. 11 Indium vs. tin for In-bearing sphalerite from worldwide deposits. Large symbols represent hand-picked sphalerite samples (< 100 g each) and ore concentrates, whereas small symbols stand for median values of EPMA or LA-ICP-MS spot measurements on sphalerite. Data are from Stedingk (1993), Cook et al. (2009), Ishihara et al. (2011), Murakami and Ishihara (2013), Dill et al. (2013), and Graupner et al. (2019). The data for Freiberg are from Bauer et al. (2019a) and are plotted (crosses) for Fe-rich sphalerite Ia (sph Ia; from kb veins), Fe-rich sphalerite Ib (sph Ib; from eb veins), and coarse-grained sphalerite IIb (sph IIb; from fba veins). The dashed circle around the sph Ia symbol stands for the range for individual sph Ia samples. *Based on median values for deposits studied by Cook et al. (2009)

the In-enriched ore minerals (mostly sphalerite; Fig. 11) or bound to discrete Sn minerals in the ore veins (cassiterite, stannite). Discrete In-bearing mineral phases (e.g., roquesite, sakuraiite) are typical of such veins (Cook et al. 2009; Dill et al. 2013; Murakami and Ishihara 2013).

The contrasting features between Sn-In-rich vein-type systems worldwide and Lautenthal can be discussed using the Freiberg district in the Variscan Orogen (Erzgebirge, Germany). In contrast to Lautenthal, the Freiberg vein systems are affected by magmatic-hydrothermal fluids from post-collisional lamprophyric and rhyolitic dikes (Seifert and Sandmann 2006). Such fluids are likely, but could not be proven in Freiberg so far (Swinkels et al. 2022). Sphalerite Ia from the Zn-Sn-Cu sequence ("indium stage") of the polymetallic-sulfide-quartz ("kb") formation is the main host for In in Freiberg with median In contents of 424 ppm (In_{max}, 2680 ppm), median Ga contents of 6 ppm (Ga_{max}, 180 ppm), and median Sn contents of 36 ppm (Sn_{max}, 7640 ppm; Bauer et al. 2019a; Fig. 11). Bulk ore geochemistry of "kb" veins shows high Sn concentrations with a mean of 1500 ppm Sn (Sn_{max}, 1.3 wt%; Seifert and Sandmann 2006). The In concentrations in sphalerite Ia from Freiberg are similar to the In-enriched sphalerite-2b of the carbonate-sulfide stage at Lautenthal with median In contents of 250 ppm (In_{max}, 3400 ppm); however, the median Ga contents are higher (165 ppm; Ga_{max}, 1200 ppm) and the median Sn contents lower (13.5 ppm; Sn_{max}, ~ 450 ppm) at Lautenthal (Table ESM 2; Fig. 7), when comparing these two sphalerite generations directly. The temperature conditions during formation of the Freiberg "kb" formation clearly exceeded 300 °C and a genetic link between In- and Sn-bearing fluids is indicated (Seifert and Sandmann 2006). In contrast to Freiberg, the hydrothermal ore system at Lautenthal is low in Sn with even its highest enrichments in hand-picked In-rich (~ 380 ppm) concentrates never exceeding 30 ppm Sn (Table 3), and the ore formation temperatures are lower.

The In-rich ore type of the Lautenthal deposit neither spatially nor temporally shows a direct link to magmatic-hydrothermal processes. The Sn-poor nature of its ore forms a significant difference to the In-rich vein-like mineralization styles known from other parts of the world. This is probably due to the lack of magmatic input during ore formation in the Upper Harz Mountains during the Mesozoic. One model for the source(s) of the base metals in the Harz vein district based on, e.g., Pb isotopic compositions of galena, Sr isotopic compositions of calcite, and fluid inclusion data, assumes a crustal source involving a pile of deep-seated unmetamorphosed or very-low-grade metamorphic Paleozoic sediments of varied lithologies (Lévêque and Haack 1993a, b; Lüders et al. 1993a; de Graaf et al. 2020), with metals extracted by interaction with circulating basement brines of probably metamorphic origin (Nadoll et al. 2019 and references therein).

Summary and conclusions

(1) Massive, banded, and breccia ore types of main ore stage I (quartz-sulfide stage) of the hydrothermal Lautenthal base metal vein deposit contain sphalerite-1-galena-1-quartz associations with accessory Fe-Co-rich gersdorffite-1, whereas the breccia ore of main ore stage II (carbonate-sulfide stage) is mainly composed of sphalerite-2-galena-2-carbonate/quartz associations with accessory Sb-rich gersdorffite-2.

(2) The moderate Fe-bearing sphalerite-1 hosts low In, moderate Ga, and very low Sn contents with median LA-ICP-MS values of 0.3 ppm, 31.5 ppm, and below LOD, respectively. Sphalerite-1 sometimes shows overprinting textures, replacement by chalcopyrite, and a related increase in its In contents. The Fe-poor sphalerite-2b hosts higher In and Ga contents and slightly enriched Sn with median values of 250 ppm, 165 ppm, and 13.5 ppm, respectively. Very high In values for individual locations (median, 574 ppm; In_{max}, 3400 ppm) occur restricted to sphalerite-2b. Median Ge contents are low for both sphalerite generations (7.4–9.2 ppm).

(3) Lateral geochemical and temperature zonation for main ore stage I is taken into consideration based on observed systematic changes in the calculated sphalerite-1 GGIMFis temperatures along the Lautenthal fault zone and geological data as well as strongly variable frequencies and crystal sizes of gersdorffite-1. GGIMFis temperature estimates for sphalerite-1 (median) are ~ 230 °C for the Lautenthal orebody and ~ 175 °C for the Bromberg orebody. Sphalerite-2 data indicate formation temperatures of ~ 185 °C (median).

(4) To scale-up the micro-analytical data, bulk compositions of hand-picked sphalerite samples and sphalerite ore concentrates were determined. Two hand-picked sphalerite-2b samples from the Bromberg orebody contained ~ 380 ppm In with In/Zn, ~ 0.70×10^{-3}. Moderate volume concentrates (~ 1–50 kg each) from the same location, which are composed of a mixture of ores from main ore stages I and II, contained 66 to 109 ppm In and 54 to 65 ppm Ga.

(5) The results of this work demonstrate that formation of vein-style In-bearing sphalerite mineralization is also possible without a magmatic-hydrothermal system. This In mineralization type has the diagnostic feature of low Sn content.

Supplementary Information The online version contains supplementary material available at https://doi.org/10.1007/s00126-024-01261-8.

Acknowledgements The results of this study contribute to the BGR project "RoStraMet" and the r^4-research project HTMET. The authors are grateful to C. Möhler and the team of the visitors mine Lautenthal's Glück for their active support of the field work and sampling campaign in their mine. The team of the Höhlen- und Grubenrettung Harz is thanked for logistic support of the underground work in the abandoned mine workings. D. Henry and A. Heiner are thanked for sample preparation and C. Grisat for compilation of drill core chemical data. Analytical support on the LA-ICP-MS, µ-EDXRF, and electron microprobe analyses by H.-E. Gäbler, D. Rammlmair, W. Nikonow, D. Göricke, and C. Wöhrl is greatly appreciated. A. Haas is thanked for analytical work. U. Schwarz-Schampera, F. Melcher, H. Dill, J. Alles, V. Lüders, H. Franke, and B. Nawothnig are thanked for fruitful discussions. The manuscript benefitted strongly from the comments of two anonymous reviewers and the editors of Mineralium Deposita A. Müller and B. Lehmann.

Funding Open Access funding enabled and organized by Projekt DEAL. The BGR authors thank the German Federal Ministry of Education and Research (BMBF) for the financial support (FKZ: 033R131A).

Declarations

Conflict of interest The authors declare no competing interests.

Disclaimer All authors certify that they have no affiliations with or involvement in any organization or entity with any financial interest or non-financial interest in the subject matter or materials discussed in this manuscript. The authors have no financial or proprietary interests in any material discussed in this article.

References

Barton PB, Bethke PM (1987) Chalcopyrite disease in sphalerite: pathology or epidemiology. Amer Mineral 72:451–467

Bauer ME, Burisch M, Ostendorf J, Krause J, Frenzel M, Seifert T, Gutzmer J (2019a) Trace element geochemistry of sphalerite in contrasting hydrothermal fluid systems of the Freiberg district, Germany: insights from LA-ICP-MS analysis, near-infrared light microthermometry of sphalerite-hosted fluid inclusions, and sulfur isotope geochemistry. Miner Deposita 54:237–262. https://doi.org/10.1007/s00126-018-0850-0

Bauer ME, Seifert T, Burisch M, Krause J, Richter N, Gutzmer J (2019b) Indium-bearing sulfides from the Hämmerlein skarn deposit, Erzgebirge, Germany: evidence for late-stage diffusion of indium into sphalerite. Miner Deposita 54:175–192. https://doi.org/10.1007/s00126-017-0773-1

Baumann A, Grauert B, Mecklenburg S, Vinx R (1991) Isotopic age determinations of crystalline rocks of the Upper Harz Mountains, Germany. Geol Rundsch 80:669–690

Behr HJ, Gerler J, Horn EE, Reutel C (1987) Ergebnisse zur Gangtektonik und hydrothermalen Mineralisation im Mittel- und Oberharz aus der Untersuchung von Flüssigkeitseinschlüssen. Fortschr Miner 65, Beiheft 1:19

Bente K, Doering T (1993) Solid-state diffusion in sphalerites: an experimental verification of the "chalcopyrite disease." Eur J Miner 5:465–478

Boness M, Haack U, Feldmann KH (1990) Rb/Sr-Datierung der hydrothermalen Pb-Zn-Vererzung von Bad Grund (Harz), BRD. Chem Erde 50:1–25

Brauer S (2013) Geochemische Analysen repräsentativer Erzproben der Lagerstätte Rammelsberg. MSc thesis, TU Clausthal, Clausthal-Zellerfeld, 39 pp. (in German)

Brinckmann J, Brüning U, Hinze C, Stoppel D (1986) Das Bundesbohrprogramm im West-Harz – Paläogeographische Ergebnisse (The federal drilling program in the Western Harz – paleogeographical results). Geol Jahrb D78:5–58 (in German with English abstract)

Buschendorf F, Hüttenhain H (1971) Allgemeiner Überblick über den Aufbau und Inhalt der Blei-Zink-Erzgänge (General overview over the tectonics and mineral composition of the lead-zinc ore veins). Beihefte Geol Jahrb 118:52–82 Hannover (in German)

Buschendorf F, Dennert H, Hannak W, Hüttenhain H, Mohr K, Sperling H, Stoppel D (1971) Die Blei-Zink-Erzgänge des Oberharzes (The lead-zinc ore veins of the Upper Harz mountains). Beihefte Geol Jahrb 118, Hannover, 211 p (in German with English summary)

Cook NJ, Ciobanu CL, Pring A, Skinner W, Shimizu M, Danyushevsky L, Saini-Eidukat B, Melcher F (2009) Trace and minor elements in sphalerite: a LA-ICPMS study. Geochim Cosmochim Acta 73:4761–4791

Cook NJ, Sundblad K, Valkama M, Nygard R, Ciobanu CL, Danyushevsky L (2011) Indium mineralization in A-type granites in southeastern Finland: insights into mineralogy and partitioning between coexisting minerals. Chem Geol 284:62–73

de Graaf S, Lüders V, Banks D, Sosnicka M, Reijmer JJG, Kaden H, Vonhof HB (2020) Fluid evolution and ore deposition in the Harz Mountains revisited: isotope and crush-leach analyses of fluid inclusions. Miner Deposita 55:47–62

Dill HG (2015) The Hagendorf-Pleystein province: the center of pegmatites in an ensialic orogen. Switzerland Springer Cham, Heidelberg, New York, p 475

Dill HG, Garrido MM, Melcher F, Gomez MC, Weber B, Luna LI, Bahr A (2013) Sulfidic and non-sulfidic indium mineralization of the epithermal Au–Cu–Zn–Pb–Ag deposit San Roque (Provincia Rio Negro, SE Argentina) — with special reference to the "indium window" in zinc sulfide. Ore Geol Rev 51:103–128. https://doi.org/10.1016/j.oregeorev.2012.12.005

Franke W, Oncken O (1995) Zur prädevonischen Geschichte des Rhenohercynischen Beckens. Nova Acta Leopoldina NF 71(291):53–72 (in German)

Franke, W (2000) The mid-European segment of the Variscides: tectonostratigraphic units, terrane boundaries and plate tectonic evolution. – In: Franke, W, Haak, V, Oncken, O, Tanner, D (eds): Orogenic Processes: Quantification and Modelling in the Variscan Belt: 35–62, London (Geological Society Special Publications)

Frenzel M, Hirsch T, Gutzmer J (2016) Gallium, germanium, indium, and other trace and minor elements in sphalerite as a function of deposit type – a meta-analysis. Ore Geol Rev 76:52–78

Gabert G (1958) Petrologische Beziehungen des Oberharzer Kersantites zu Gang- und Tiefengesteinen des Harzes. Geol Jahrb 75:79–114

Graupner T, Zeller T, Goldmann D, Kammer U, et al. (2019) Hochtechnologie-relevante Metalle in deutschen sulfidischen

Buntmetallerzen – Ressourcenpotenzialabschätzung (HTMET). Final report of the r^4-project. Hannover. 133 pp. (in German)
Haack U, Lauterjung J (1993) Rb/Sr dating of hydrothermal overprint in Bad Grund by mixing lines. Monogr Ser Mineral Deposits 30:103–113
Haas A (2020) Vergleichende Untersuchungen zur Aufbereitung komplexer, sondermetallhaltiger Sulfiderze mittels Flotation und hydrometallurgischer Verfahren im Hinblick auf eine optimierte Wertstoffgewinnung. PhD thesis, TU Clausthal, Clausthal-Zellerfeld. 137 pp. (in German)
Hall JR (2019) Mineralogisch-lagerstättenkundliche Untersuchungen an arsenidischen Nickelerzen aus dem nördlichen Oberharz. BSc thesis, TU Clausthal, Clausthal-Zellerfeld, 55 pp. (in German)
Henning S, Birkenfeld S, Graupner T, Franke H, Nawothnig B, Pursche K (2019) The new critical metals database "HTMET": high tech trace element characteristics of sulphides from base metal provinces in the Variscan basement and adjacent sedimentary rocks in Germany. Z Dtsch Ges Geowiss 170:161–180
Henning S, Graupner T, Krassmann T, Gäbler H-E, Goldmann S, Kus J, Onuk P (2022) Processes of enrichment of trace metals for high tech applications in hydrothermal veins of the Ruhr Basin and the Rhenish Massif, Germany. Can Mineral 60:881–912
Huckriede H, Wemmer K, Ahrendt H (2004) Paleogeography and tectonic structure of allochthonous units in the German part of the Rheno-Hercynian Belt (Central European Variscides). Int J Earth Sci 93:414–431
Ishihara S, Hoshino K, Murakami H, Endo Y (2006) Resource evaluation and some genetic aspects of indium in the Japanese ore deposits. Resource Geol 56(3):347–364
Ishihara S, Murakami H, Marquez-Zavalia MF (2011) Inferred indium resources of the Bolivian tin-polymetallic deposits. Resource Geol 61:174–191
Jacobsen W, Schneider H, Sperling H, Tiemann KC (1971) Übersichtskarte der Gangzüge und Gänge im nordwestlichen Oberharz, Beihefte Geol Jahrb 118, Map 34 (in German)
Jacobsen W, Schneider H (1951) Die Erzgänge des nordwestlichen Oberharzes. Eine Erläuterung zur Gangkarte 1:25 000. Geol Jahrb 65:707–768
Johan Z (1988) Indium and germanium in the structure of sphalerite: an example of coupled substitution with Copper. Mineral Petrol 39:211–229. https://doi.org/10.1007/bf01163036
Jovic S, Lopez L, Guido D, Redigonda J, Paez G (2015) Indium mineralization in epithermal polymetallic deposits of Patagonia, Argentina. In: Andre-Mayer AS, Cathelineau M (eds) Mineral resources in a sustainable world. Society for geology applied to mineral deposits, Nancy France, pp 785–786
Klemm DD (1965) Syntheses and analyses in the ternary plots FeAsS-CoAsS-NiAsS and FeS_2-CoS_2-NiS_2. Neues Jb Miner Abh 103:205–255 (in German with English abstract)
Klockmann F (1893) Uebersicht über die Geologie des nord-westlichen Oberharzes (Overview on the geology of the north-western part of the Upper Harz Mts). Z Dt Geol Ges XLV:253–287 (in German)
Korges M, Weis P, Lüders V, Laurent O (2020) Sequential evolution of Sn–Zn–In mineralization at the skarn-hosted Hämmerlein deposit, Erzgebirge, Germany, from fluid inclusions in ore and gangue minerals. Miner Deposita 55:937–952. https://doi.org/10.1007/s00126-019-00905-4
Kraume E (1958) Zur Frage der Mineralisierung der Oberharzer Erzgänge in größerer Teufe (About the mineralization of the ore veins in the Upper Harz in greater depth). Zeitschrift Fuer Erzbergbau Und Metallhuettenwesen 11:257–263 (in German)
Kraume E (1955) Die Erzlager des Rammelsberges bei Goslar (The orebodies of the Rammelsberg near Goslar). Beihefte Geol Jahrb 18, 394 p (in German)
Kraume E (1964) Der Schleifsteintaler Gangzug (The Schleifsteintaler vein zone). PREUSSAG Metall. Unpublished report, Goslar, 12.05.1964. 59 pp. (in German)
Kumar AA, Sanislav IV, Dirks PHGM (2022) The geological setting of the indium-rich Baal Gammon and Isabel Sn-Cu-Zn deposits in the Herberton Mineral Field, Queensland. Australia. Ore Geol Rev 149:105095. https://doi.org/10.1016/j.oregeorev.2022.105095
Kumar AA, Sanislav IV, Cathey HE, Dirks PHGM (2023) Geochemistry of indium in magmatic-hydrothermal tin and sulfide deposits of the Herberton Mineral Field, Australia. Miner Deposita 58:1297–1316. https://doi.org/10.1007/s00126-023-01179-7
Lepetit P, Bente K, Doering T, Luckhaus S (2003) Crystal chemistry of Fe-containing sphalerites. Phys Chem Miner 30:185–191
Lévêque J, Haack U (1993a) Pb isotopes of hydrothermal ores in the Harz. Monogr S Mineral Deposits 30:197–210
Lévêque J, Haack U (1993b) Sr isotopes in calcites of hydrothermal veins in the Harz and possible sources of solutions. Monogr S Mineral Deposits 30:159–168
Lüders V, Ebneth J (1993) Sulfur isotopes in shales and their relation to vein sulfides (and barite) of the Upper and Middle Harz Mountains. Monogr S Mineral Deposits 30:231–240
Lüders V, Möller P (1992) Fluid evolution and ore deposition in the Harz Mountains. Eur J Miner 4:1053–1068
Lüders V, Gerler J, Hein UF, Reutel C (1993a) Chemical and thermal development of ore-forming solutions in the Harz Mountains: a summary of fluid inclusion studies. Monogr S Mineral Deposits 30:117–132
Lüders V, Stedingk K, Franzke HJ (1993b) Review of geological setting and mineral paragenesis. Monogr S Mineral Deposits 30:5–11
McKerrow WS, MacNiocaill C, Ahlberg PE, Clayton G, Cleal CJ, Eagar RMC (2000) The Late Palaeozoic relations between Gondwana and Laurussia. In: Franke W, Haak V, Oncken O, Tanner D (eds), Orogenic Processes: Quantification and Modelling in the Variscan Belt. Geological Society Special Publication 179, pp 9–20
Möller P, Lüders V (1993) Synopsis. Monogr S Mineral Deposits 30:285–291
Möller P, Morteani G, Dulski P (1984) The origin of the calcites from Pb-Zn veins in the Harz Mountains, Federal Republic of Germany. Chem Geol 45:91–112. https://doi.org/10.1016/0009-2541(84)90117-7
Müller AG (2022) The Rammelsberg shale-hosted Cu-Zn-Pb sulfide and barite deposit, Germany: linking SEDEX and Kuroko-type massive sulfides – slide presentation and explanatory notes, Version 2. Society for Geology Applied to Mineral Deposits (SGA), www.e-sga.org, Publications, Mineral Deposit Archive
Murakami H, Ishihara S (2013) Trace elements of Indium-bearing sphalerite from tin-polymetallic deposits in Bolivia, China and Japan: a femto-second LA-ICPMS study. Ore Geol Rev 53:223–243. https://doi.org/10.1016/j.oregeorev.2013.01.010
Nadoll P, Sosnicka M, Kraemer D, Duschl F (2019) Post-Variscan structurally-controlled hydrothermal Zn-Fe-Pb sulfide and F-Ba mineralization in deep-seated Paleozoic units of the North German Basin: A review. Ore Geol Rev 106:273–299
Nikonow W, Rammlmair D (2017) Automated mineralogy based on energy dispersive X-ray fluorescence microscopy (μ-EDXRF) applied to plutonic rock thin sections in comparison to Mineral Liberation Analyser. Geosci Instrum Method Data Syst 6:429–437. https://doi.org/10.5194/gi-6-429-2017
Sahlström F, Arribas A, Dirks P, Corral I, Chang Z (2017) Mineralogical distribution of germanium, gallium and indium at the Mt Carlton high-sulfidation epithermal deposit, NE Australia, and comparison with similar deposits worldwide. Minerals 7(11):213. https://doi.org/10.3390/min7110213

Schirmer T, Ließmann W, Macauley C, Felfer P (2020) Indium and antimony distribution in a sphalerite from the "Burgstaetter Gangzug" of the Upper Harz Mountains Pb-Zn mineralization. Minerals 10(9):791. https://doi.org/10.3390/min10090791

Schriel W (1954) Die Geologie des Harzes. Schriften der wirtsch.-wiss. Gesellschaft zum Studium Niedersachsens, NF 49, Hannover, 308 p (in German)

Schwarz-Schampera U (2014) Indium. In: Gunn G (ed) Critical Metals Handbook. John Wiley & Sons, Ltd., Chichester, UK, pp 204–229

Schwarz-Schampera U, Herzig P (2002) Indium: geology, mineralogy, and economics. Springer Verlag, Berlin, Germany

Seifert T, Sandmann D (2006) Mineralogy and geochemistry of indium-bearing polymetallic vein-type deposits: Implications for host minerals from the Freiberg district, Eastern Erzgebirge, Germany. Ore Geol Rev 28:1–31

Sinclair WD, Kooiman GJA, Martin DA, Kjarsgaard IM (2006) Geology, geochemistry and mineralogy of indium resources at Mount Pleasant, New Brunswick. Ore Geol Rev 28:123–145

Sperling H (1973) Die Erzgänge des Erzbergwerks Grund (The ore veins of the mine of Grund (Silbernaaler Gangzug, Bergwerksglücker Gang and Laubhütter Gang)). Geol Jahrb D 2:3–205 (in German with English abstract)

Sperling H (1979) Silbernaler Gangzug (The Silbernaal vein zone). Geol Jahrb D 34:18–77 (in German with English abstract)

Sperling H, Berthold D (1979) Schleifsteintaler Gangzug (The Schleifsteintal vein zone). Geol Jahrb D 34:272–282 (in German with English abstract)

Sperling H, Stoppel D (1979) Lautenthaler Gangzug (The Lautenthal vein zone). Geol Jahrb D 34:225–246 (in German with English abstract)

Stedingk K (1986) Der Kahlebergsandstein in den Bohrungen Adlersberg, Spiegeltal und Eselsberg (West-Harz) (The Kahleberg sandstone in the Adlersberg, Spiegeltal and Eselsberg boreholes (Northwestern Harz Mts). Geol Jahrb D 78:79–94 (in German with English abstract)

Stedingk K (1993) The West Field Ore Body II of the Bad Grund mine: a case study. Monogr S Mineral Deposits 30:55–64

Stedingk K (2021) Bilanz und Perspektiven der Harzer Erzlagerstättenforschung - Fakten und Schlussfolgerungen. In: Juranek C, Knolle F (eds) Bilanz und Perspektiven der Harz-Forschung - 150 Jahre Harz-Verein für Geschichte und Altertumskunde, Part II, Harz-Forschungen 34. Berlin, Wernigerode (in German), pp 24–91

Stedingk K (1982) Die Mineralisation des Kahlebergsandsteinkomplexes im Umfeld der Rammelsberger Lagerstätte. (The mineralization of the Kahleberg sandstone complex close to the Rammelsberg deposit). PhD thesis, TU Clausthal, 67 pp. and 87 figures (in German)

Stedingk K (2012) Geologie und Erzlagerstätten im Oberharz (Geology and ore deposits in the Upper Harz Mts.). In: Stedingk K, Kleeberg K (eds) Exk Fü Veröff Dt Ges Geowiss 247:9–81 (in German)

Stoppel D, Gundlach H, Heberling E (1983) Schwer- und Flußspatlagerstätten des Südwestharzes (Barite and fluorite deposits in the southwestern Harz Mountains). Geol Jahrb D 54, 269 p (in German with English abstract)

Swinkels LJ, Schulz-Isenbeck J, Frenzel M, Gutzmer J, Burisch M (2022) Spatial and temporal evolution of the Freiberg epithermal Ag-Pb-Zn district, Germany. Econ Geol 116:1649–1667

von Eynatten H, Voigt T, Meier A, Franzke H-J, Gaupp R (2008) Provenance of Cretaceous clastics in the Subhercynian Basin: constraints to exhumation of the Harz Mountains and timing of inversion tectonics in Central Europe. Int J Earth Sci 97:1315–1330

Wagner T, Cook N (1997) Mineral reactions in sulphide systems as indicators of evolving fluid geochemistry- a case study from the Apollo mine, Siegerland, FRG. Mineral Mag 61:573–590

Weber J (2013) Mineralogische und geochemische Untersuchungen an ausgewählten Vererzungen des Lautenthaler und Bockswieser Reviers im Oberharz (Mineralogical and geochemical studies on selected ore occurrences of the Lautenthal and Bockwiese mine districts in the Upper Harz). MSc thesis, TU Clausthal, 35 pp. and 28 figures (in German)

Zech J, Jeffries T, Faust D, Ullrich B, Linnemann U (2010) U/Pb-dating and geochemical characterization of the Brocken and the Ramberg Pluton, Harz Mountains. Germany. Geologica Saxonica 56(1):9–24